

Cite this: *J. Mater. Chem. B*, 2022,  
10, 2357Received 20th November 2021,  
Accepted 26th January 2022

DOI: 10.1039/d1tb02549j

rsc.li/materials-b

## Engineering surface patterns on nanoparticles: new insights into nano-bio interactions

Boyang Hu,<sup>†ab</sup> Ruijie Liu,<sup>†c</sup> Qingyue Liu,<sup>†ac</sup> Zi'an Lin,<sup>b</sup> Yiwei Shi,<sup>b</sup> Jun Li,<sup>b</sup>  
Lijun Wang,<sup>ac</sup> Longjie Li,<sup>\*ac</sup> Xianjin Xiao<sup>id</sup><sup>\*c</sup> and Yuzhou Wu<sup>id</sup><sup>\*b</sup>

The surface properties of nanoparticles affect their fate in biological systems. Based on nanotechnology and its methodology, pioneering studies have explored the effects of chemical surface patterns on the behavior of nanoparticles and provided many new insights into nano-bio interfaces. In this review, we would like to provide a summary of how the nanoparticle surface pattern modulates its biological effects. The relationship between the surface pattern of nanoparticles and the generated interaction with cell membranes, recognition of viruses and adsorption of proteins was discussed. On this basis, we believe that a reasonable design of the surface microstructure will promote the application of artificial nanoparticles in biomedicine and provide a new strategy for improving the design of nano-drug carriers.

### 1. Introduction

The surface properties and patterns of nanoparticles significantly affect their interactions with biomolecules, cells and microorganisms.<sup>1–4</sup> Nanoparticles with a positively charged or negatively charged surface display distinct cell uptake efficiency and tissue distribution, while the hydrophilicity of nanoparticles also determines their blood circulation, tissue penetration and protein corona adsorption.<sup>5</sup> In most studies, the surface chemical properties of synthetic nanoparticles are often presumed to be homogenous. However, in nature, the biorecognition between biomolecules and nanostructures are obviously more complicated compared to synthetic systems. The surface patterns of recognition partners perfectly match with each other with multiple interactions involved, which is essential for the extraordinary specificity.<sup>6–9</sup>

Recently, the advancement of nanofabrication methods allowed creation of nanoparticles with heterogeneous surface patterns, which provide opportunities for fine-tuning and a deeper understanding of nano-bio interactions. The engineered surface patterns starting from “Janus” particles with two phases separated have been further developed to multiple patches with desired geometry and even regular strips.<sup>3,10</sup> The recent emerging DNA nanotechnology

even enabled precise surface pattern design at pre-encoded positions.<sup>7,11–13</sup> Based on these techniques, pioneering studies have explored how chemical surface patterns would influence the nanoparticle behavior in biological systems and provided numerous new insights into the nano-bio interface. These findings are crucial for promoting the biomedical applications of nanoparticles and provided new strategies to improve the design of nanocarriers.<sup>3,14–16</sup>

In this review, by merging the most recent developments in both nanofabrication strategies to create fine surface patterns and the biological understanding of surface pattern driving biorecognition, we intend to provide more perspectives on how to design surface patterns on nanoparticles to tune their biological effects. The nanoparticles discussed herein are less than 1 μm in diameter considering their potential in nanomedicine, and the surface patterns refer to more than two distinct chemical compositions regularly arranged on the particle surface instead of the statistical mix. The synthetic methods will be firstly summarized, and the relation between surface patterns on nanoparticles and the resulting cell membrane interactions, protein corona adsorption and virus recognition would be further discussed in detail (Scheme 1). We believe that the current knowledge in this field is just a prelude, and the limitations and further potential will be particularly deliberated.

### 2. Biorecognition of natural molecules and artificial nanoparticles

#### 2.1 Mechanism of biorecognition in nature

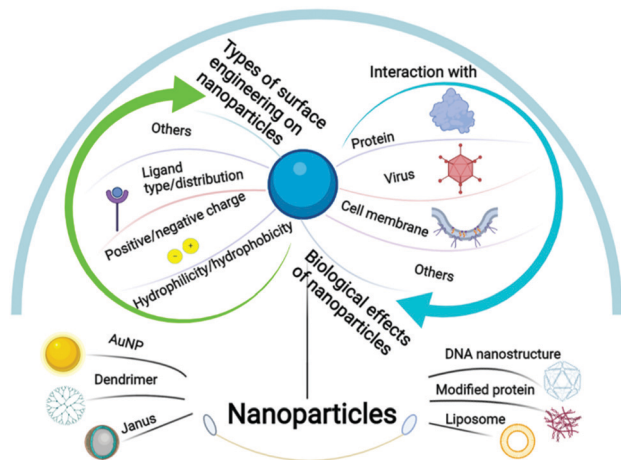
Accurate recognition between biological molecules is the basis for the development of organisms. Both general and specific

<sup>a</sup> School of Life Science and Technology, Wuhan Polytechnic University, Wuhan 430023, China. E-mail: lilongjie@whpu.edu.cn

<sup>b</sup> Hubei Key Laboratory of Bioinorganic Chemistry and Materia Medica, Hubei Engineering Research Center for Biomaterials and Medical Protective Materials, School of Chemistry and Chemical Engineering, Huazhong University of Science and Technology, Wuhan 430074, China. E-mail: wuyuzhou@hust.edu.cn

<sup>c</sup> Institute of Reproductive Health, Tongji Medical College, Huazhong University of Science and Technology, Wuhan 430030, China. E-mail: xiaoxianjin@hust.edu.cn

† These authors contributed equally to this work.



**Scheme 1** Schematic illustration of the species, types of surface engineering and the biological effects of nanoparticles covered in this review.

interactions occur among many important biological macromolecules, including polysaccharides, proteins, enzymes, and nucleic acids. Intercellular recognition can be achieved by selectively combining surface molecules with the corresponding active substances or signalling molecules, such as protein ion channels, and recognition between antigens and antibodies.<sup>17–20</sup> Macrophages recognise aging cells through “eat me” and “don’t eat me” signalling molecules. T cells recognise tumour cells through T cell receptors (TCR), tumour antigens, and MHC molecules. Lipopolysaccharides (LPS) induce inflammatory responses in immune cells by interacting with Toll-like receptor-4 (TLR-4). Therefore, the interactions between biological macromolecules (*e.g.*, proteins, lipids, and polysaccharides) provide a molecular basis for the recognition and cognition of organisms.<sup>21–23</sup>

In nature, the first step of mutual recognition between biomolecules is the structural complementarity of the binding sites of the two molecules, and the second is the generation of sufficient chemical forces between the binding sites. Berger and Milstein *et al.* found that conformational selection is one of the reasons for the formation of antigen–antibody complexes.<sup>24–26</sup> Molecules undergoing molecular recognition exist in the form of conformational complexes. When the ratio of ligands bound by preferentially recognized molecular conformation is reduced, other molecular conformations will change to preferentially bound molecular conformations.<sup>24</sup> Chemical forces are mainly van der Waals, hydrogen bond, hydrophobic and electrostatic forces, which arise from the interaction between various conformations.<sup>25</sup> Additionally, the charge will affect the recognition and binding of natural biomolecules to a certain extent, such as homogalacturonan (HG) with a low degree of esterification (DE) and chitosan—chitosan with a positive charge in the spatial structure can interact with the carboxyl groups on HG with a low DE.<sup>27</sup> Hydrophilicity will also have a certain impact. Common carbohydrates can form a certain hydrophilic or hydrophobic region due to their functional groups and then interact with

biomolecules through hydrophilic forces (hydrogen bonds) or hydrophobic forces (hydrophobic bonds). For example, Zeng *et al.* found that azides, alkynes, ketones or aldehydes can interact with glycoproteins on the cell surface.<sup>28,29</sup> Moreover, the interaction between biomolecules and cells also relies on chemical forces such as hydrogen bonds and van der Waals forces. The polysaccharides in the cell wall rely on these weak interactions to arrange tightly, limiting the accessibility of the antibodies to the epitopes. The charged molecules can produce strong polar interactions with the phage, thereby affecting the binding of the antibody to the phage capsid protein in the phage display.<sup>25</sup> Cell–cell interactions, such as cell fusion and cell adhesion, are essentially the result of the regulation of cell membranes through chemical forces. Myoblast fusion is a multi-step process involving cell recognition and adhesion, actin cytoskeletal rearrangements, fusogen engagement, lipid mixing and fusion pore formation, ultimately resulting in the integration of two fusion partners.<sup>30</sup> This process involves the interaction of many biological molecules such as cell adhesion molecules, adaptor proteins, vesicle trafficking proteins and lipids.<sup>31</sup> During the membrane fusion process, hydrophilic lipid heads with the same charge will repel each other due to electrostatic forces.<sup>32</sup> Many life activities in nature are closely related to this, such as virus infection, cell migration, vesicle transportation, and fertilization.<sup>33</sup>

Due to the different chemical properties and physical states of different proteins and lipids on the membrane, based on hydrophobic interactions, electrostatic interactions, van der Waals forces, hydrogen bonds and hydration forces, the membrane surface will form a variety of synergistic lipid raft–protein structure domains (surface pattern). These surface patterns are critically important in mediating life activities.<sup>22</sup> For example, cholesterol-rich lipid domains play an important role when *Francisella* recognizes and infects host cells.<sup>34</sup> The lipid–protein pattern formed by the recruitment of the liganded GPI (glycosylphosphatidylinositol)-anchored receptor is very important in specific downstream signal transduction.<sup>35</sup> The internalization process mediated by caveolin-1 is also inseparable from the formation of lipid raft-related patterns.<sup>36</sup> In conclusion, although the mechanism of lipid domains on membranes to mediate cell functions needs further research, it is undeniable that the formation of these surface patterns occupies an important position in mediating recognition, signal transduction, pathogen invasion and other functions.

## 2.2 Interaction of nanoparticles with biological systems and the effect of their surface properties

The effect of nanoparticles on biological systems is mainly achieved through the interaction between nanoparticles and cells. The outer interface of human cells is primarily composed of bilayer lipid molecules with saccharides and proteins. Under natural conditions, biological macromolecules can activate many downstream reactions through interactions with cells, which maintain the basic functions of living organisms. Similarly, the interaction between artificial nanoparticles and cell membranes is important for achieving specific functions of

nanoparticles. The interaction between nanoparticles and proteins results in the formation of a protein corona, which can cause a downstream effect.<sup>37</sup> Nanoparticles can be internalised into cells *via* receptor/non-receptor-mediated pathways, in which a variety of enzymes and proteins are activated, including guanosine diphosphate (GDP), guanosine triphosphate (GTP), and heat shock proteins (HSP).<sup>38</sup> The high endocytosis efficiency of these molecules contributes to their potential application in drug delivery.

The surface properties of nanoparticles play a pivotal role in their interaction with cells. Researchers have paid much attention to the effects and related mechanisms of the surface properties of nanoparticles on their interaction with biological systems. Krishnendu *et al.* found that the formation of a protein corona is closely related to the hydrophilicity and hydrophobicity of nanoparticles, and that the modulation of the surface hydrophobicity of the nanoparticles can effectively reduce the recognition of plasma proteins by macrophages.<sup>39</sup> In addition, when interacting with a lipid bilayer membrane, hydrophilic nanoparticles tend to be distributed outside the membrane, while hydrophobic nanoparticles can be embedded inside and can even cause defects on the membrane, leading to bending, budding, or fission.<sup>40–43</sup> Surface charge also is a determining factor in the cellular uptake process of nanoparticles. Stronger attraction exists between negatively charged membranes and positively charged nanoparticles, which can enhance the turnover and tilt of phospholipid molecules. Therefore, in many cases, the uptake increases with the augmenting magnitude of charges.<sup>44</sup> Despite this, negatively charged nanoparticles can accumulate in the serum to a larger extent due to the relative reduction in charge-selective filtration, which results in the drug carrier having a longer retention time.<sup>45</sup>

Besides, the surface chemistry of nanoparticles (ligand type and ligand distribution) is an important factor affecting their interaction with the cell membrane. Moreover, inspired by the natural spike patterns on virus capsids, researchers synthesize nanoparticles with the corresponding ligand distribution, thus facilitating the interaction with a bio-interface (*e.g.* higher uptake efficiency achieved by symmetric distribution).<sup>46</sup> Since Janus nanoparticles contain heterogeneous regions, they can induce unique biological reactions, which have been widely used in drug delivery<sup>47</sup> and biological imaging.<sup>48</sup> Therefore, understanding the interaction between nanoparticles and biological interfaces and the effect of the surface patterns of nanoparticles on this interaction is of high significance for the application of nano-drugs.

### 2.3 Surface engineering on nanoparticles and the biological effect of such modifications

Nanoparticles interact *in vivo* with cells and biomolecules to produce a “nano-bio interface”. This plays a key role in the reaction of nanoparticles in biological systems. It is widely recognised that the surface properties of nanoparticles are closely related to the “nano-bio interface”. Therefore, surface engineering has emerged to change their surface properties.

Surface engineering refers to the use of physical and chemical methods to change the surface chemical properties

of particles (functional group structure, electrical, hydrophobic, and hydrophilic). In general, there are two main strategies for surface engineering: “top-down” and “bottom-up”. In the former method, various three-dimensional structures can be easily obtained by using etching technology, but the cost is high, and it is difficult to directly adjust the distance between atoms. The latter emphasises the use of smaller structural units for assembly, such as self-assembly technology with a high yield, and is the current trend in surface engineering. Based on the concept of “bottom-up” surface engineering, many chemical synthesis methods have been applied to the surface engineering of nanoparticles. The ligand-exchange method and ligand-coating method are the two most common methods used to change the surface chemistry. The former involves the substitution of ligands, which can change the nanoparticles from hydrophobic to hydrophilic, which is conducive to their participation in human body transport.<sup>49,50</sup> However, the latter focuses on implementing some groups on the nanoparticle surface. For instance, Hauck *et al.* assembled polyelectrolytes on the nanorod surface in a layer-by-layer manner.<sup>51</sup> Furthermore, the stability of nanoparticles can be maintained by surface engineering. To avoid the arbitrary absorbance by proteins, polyethylene glycol (PEG) is one of the best ligands for surface decoration. Moreover, the attachment of PEG significantly decreases the absorbance because of hydration and steric hindrance.<sup>52</sup> However, PEG has problems such as low service life caused by oxidation in the biological environment and the blood clearance effect caused by the immune system response. Zwitterionic ligands can bind water molecules effectively *via* electrostatic induced hydration, and thus the zwitterionic surface can effectively prevent protein adsorption and avoid the dilemma of PEG. Mixed-charge monolayers have been designed on the surface of nanoparticles by various methods, which expand the application of zwitterionic ligands.<sup>53,54</sup> To induce specific reactions in organisms, the corresponding ligands can be linked by covalent or non-covalent modifications to a desired location of the already modified nanoparticles.<sup>55,56</sup> Therefore, precise control of the pre-modification of these nanoparticles is essential. A monolayer can also be coated on nanoparticles, contributing to stable and multifunctional NPs because of the simultaneous use of stable and functioning ligands.<sup>57,58</sup> More importantly, these methods can be used in combination to allow the nanoparticles to respond to specific stimuli in the organism.<sup>2</sup>

Although many surface engineering methods are proposed, it is still really challenging to create the fine pattern on nanoparticles, which would rely on well-developed characterization techniques and precise control of the activities, positions and density of the functional groups.

## 3. Fine fabrication of surface patterns on nanoparticles

In this review, we mainly consider AuNPs and dendritic polymers as model particles to analyse how their surface patterns

affect their interactions with cell membranes, proteins, and viruses since they are mostly investigated at present. To form accurate surface patterns on these nanoparticles, researchers usually adopt (de)protection methods and precisely control the attributes of the core and the attached ligands. At the same time, as the modifications on emerging DNA nanomaterials are easily regulated, we will also use them as a model to discuss the interaction between ligands and receptors.

### 3.1 Construction of AuNPs with different substructures on their surfaces

AuNPs are particles with a core of gold and a radius of 1–100 nm. For decades, many methods have been proposed for their synthesis, and the shape<sup>59</sup> and size<sup>60</sup> of the AuNPs can be well controlled. Currently, researchers can obtain nanoparticles of the desired size and shape.<sup>61–64</sup> In order to exert biological effects, AuNPs can be modified in many ways to serve as a platform for linking nucleic acids, proteins, and their interactions with biological molecules or membranes, allowing them to be used for detection and drug delivery.<sup>65,66</sup> Sulphur-containing groups have been vastly used in the synthesis of gold nanoparticles because of their high affinity to gold and their ease of modification. Since the last century, researchers have developed various methods to synthesize gold nanoparticles,<sup>67,68</sup> among which the Brust–Schiffrin method, which can easily control the size and shape of the nanoparticles, is commonly used.<sup>69,70</sup>

Based on this, one of the most representative methods for further surface engineering is to add a mixed self-assembled monolayer (SAM) to a gold nanoparticle surface *via* (1) co-absorption or (2) thiol-mediated ligand substitution. This pioneering work was conducted by the Stellacci group. In 2004, they first introduced monolayer-protected gold nanoparticles with phase-separated ordered domains—the first striped-pattern nanoparticles. In their experiment, an ordered domain could be easily tailored by adjusting the radius (curvature) of the core and the octane thiol/mercaptopropionic acid ratio. In addition, they concluded that this pattern results from the thermodynamic equilibrium state, resulting in its good stability.<sup>71</sup> Subsequently, they made significant progress in synthesizing a series of other gold nanoparticles with various properties, including binary SAM gold nanoparticles, in which two opposite ligand domains are formed (Fig. 1a).<sup>72–75</sup> Moreover, the differences between “striped” and “binary” can be explained by the compatibility of the ligands—compatibility leads to a striped pattern, whereas the other leads to “binary”. Based on these observations, they proposed a theory that micro-phase separation is critical to determine the final morphology. For striped gold nanoparticles, the increase in entropy by conformational changes is of high importance. Only when it overcomes the penalty of enthalpy by complete phase separation, a striped pattern occurs, heavily relying on the particle size, *i.e.* a small radius would give rise to the formation of Janus rather than a striped pattern.<sup>75,76</sup>

To endow gold nanoparticles with a certain function, they can be linked with (bio)polymers. Their preparation strategies

can be divided into three types: (1) grafting from—polymerization on the particle surface during their synthesis, (2) grafting to—particles are synthesized and mixed with polymers, and (3) post-synthetic modifications. To stabilize the particles, inorganic polymers, such as PEG and PVA (polyethyleneimine), are conjugated to gold nanoparticles mostly *via* grafting from/to.<sup>77,78</sup> Biomolecules are commonly conjugated to gold nanoparticles through post-synthetic modifications. Gold nanoparticles can be easily prepared using amino acids through the formation of Au–S bonds. Combined with peptides or metal ions, they have been applied in biosensing and molecular computing.<sup>79,80</sup> Similarly, DNA undergoing the thiolate process can directly bind to gold nanoparticles aiming for diagnostics and the following construction of a nanodevice.<sup>81,82</sup>

However, observation of the dynamic process of surface pattern formation can be hardly achieved. Moreover, it is challenging to construct gold nanoparticles with a specific number of ligands, which hinders the preparation of a desirable nanopattern. Moreover, it is relatively simple to exert delicate control on the conjugation of biomolecules to gold nanoparticles. This requires the development of methods to control the thiol activity and improvements in dynamic characterization techniques of nanoparticles.

### 3.2 Construction of dendrimers with different substructures on their surface

Dendrimers are a family of nanosized three-dimensional polymers characterised by unique dendritic branching structures and compact spherical geometries. Their names come from the Greek word “dendron”, which means “tree”, and refer to the unique organisation of polymer units.<sup>83</sup> Dendritic polymers are obtained through an iterative cycle reaction, and one layer of molecules is added in each iterative cycle. There are two main strategies for synthesising dendritic polymers (Fig. 1b).<sup>16</sup> The first is the divergence method,<sup>84</sup> in which the growth of dendritic units originates from the core site (root). This method assembles monomer modules into radial and branched motifs according to certain dendritic rules and principles.<sup>85</sup> The second is the convergence method,<sup>86</sup> which starts from the molecules that are about to become the surface of the branch units (that is, from the leaves of the molecular tree) and reaches the root reaction core inward. This requires that a single reaction branch unit is formed first, and then multiple branch units react with the multifunctional core to obtain the dendritic polymer structure.<sup>16</sup>

Polyphenylene dendrimers (PPDs) are unique members of the dendrimer family, whose main chain is mainly composed of substituted benzene rings.<sup>87,88</sup> PPDs have a high extent of branching, rigidity and monodispersity. The structure of a PPD contains three levels: core, scaffold, and surface. Compared with other dendrimers, PPDs are more interesting because of their rigidity and non-conformational rearrangement. Dendrimers generally have flexible dendrimers with arms, which makes dendrimers easily undergo conformational rearrangement. Therefore, the surface of dendrimers is obscured by special functionalized sites and cannot function,



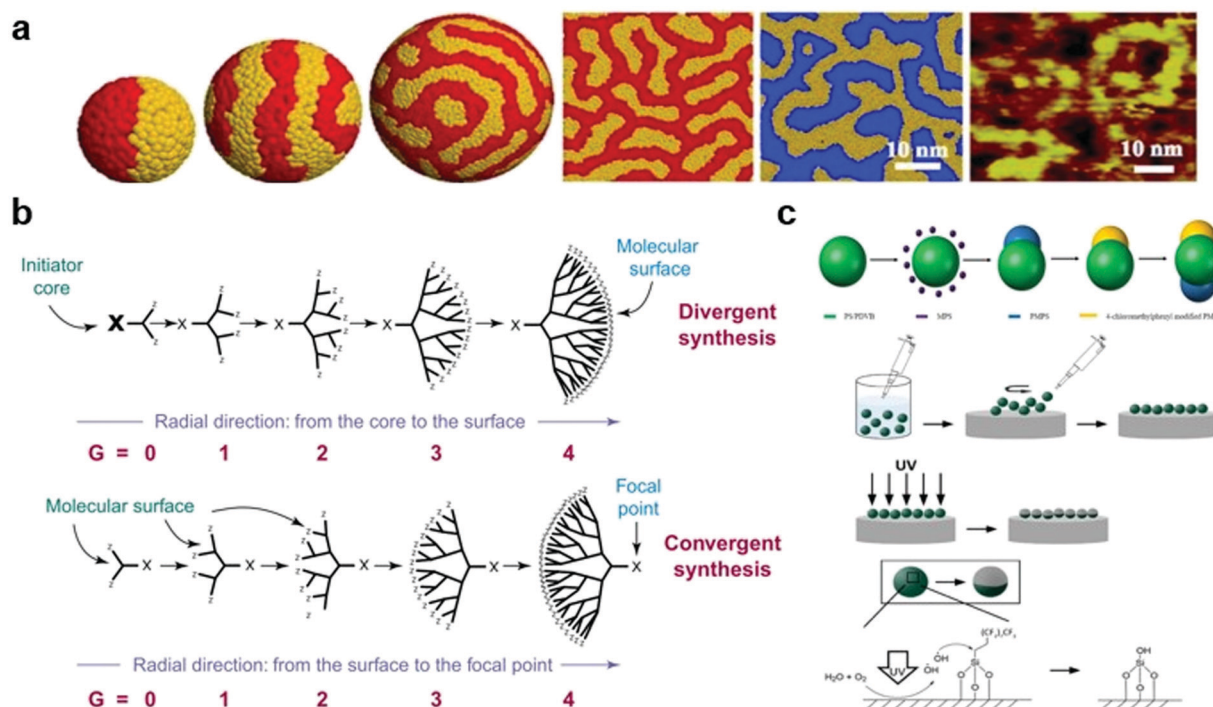


**Fig. 1** (a) Mesoscale simulation results of a fixed length ratio (4:7) on the surface of gold nanoparticles with different degrees of curvature. (b) Two principles of synthetic methods (divergent synthesis and convergent synthesis) for constructing dendritic macromolecules (dendrons). (c) Illustration of the synthesis of triblock Janus particles by seeded emulsion polymerization and UV irradiation. Reproduced with permission from ref. 75, 16 and 95, copyright (2007) American Physical Society, (2001) Elsevier and (2019) American Chemical Society.

which is not conducive to practical applications. Because the rigid main chain replaced by the benzene ring endows the PPDs with shape durability, when the core, scaffold, and special sites on the surface are chemically modified and functionalized on the nanoscale, there is no concern about the target properties of the molecule losing effect due to the negative influence brought about by conformational rearrangement.<sup>89,90</sup> The shape-persistence feature reveals additional possibilities for PPD applications in areas such as biological research, drug transport, and interface interactions.

The surfaces of PPDs can be finely regulated or modified to have two or more different characteristics, namely, the formation of patched dendrimers with different characteristics on the surface. For example, amphiphilic PPDs have both hydrophobic and hydrophilic functional groups on their surfaces. These amphiphilic PPDs play an important role in the interaction with proteins, cells, or viruses, and they exhibit low cytotoxicity *in vitro* and *in vivo*.<sup>91</sup> PPDs maintain a unique spherical structure in that solution, and a lipophilic cavity with a specific size is formed inside, which is a protein-like structure and can simulate substances such as human serum protein (HSA) to make “artificial proteins”,<sup>91</sup> suggesting that PPDs can be potential carriers of lipophilic drugs. Highly branched, persistent-shaped, monodisperse PPDs consist of a core, a scaffold, and a surface. The core controls and determines the number and geometry of the dendrimers of macromolecules.<sup>92,93</sup> Building blocks control the chemical functionalization and properties of the scaffold and surface.

The difference in the core or building block type affects the shape and properties of the dendrimer.

PPDs have a rigid, designable surface and a special lipophilic cavity inside, and can interact with cell membranes and viruses. These characteristics provide a broad prospect for the research and application of PPDs. Through the Diels–Alder cycle addition reaction, researchers can prepare various PPDs with different shapes and surface characteristics to explore the interaction between nanoparticles and biological interfaces.

### 3.3 Construction of “Janus” nanoparticles

Since the concept of Janus nanoparticles (NPs) was first proposed in 1991, research on them has become a hot topic in the field of biochemistry.<sup>94</sup> Janus NPs, named after a double-faced Roman God, can be defined as particles with a fine structure consisting of two or more components with different (usually opposite) physical and chemical properties. Due to their unique optical and magnetic properties, Janus NPs have high potential for biopharmaceutical and imaging applications. Similarly, there are two preparation strategies for Janus NPs, “additive” and “subtractive” (Fig. 1c).<sup>95</sup> The “additive” strategy is commonly used, including in self-assembly, seed emulsion polymerisation, and phase separation. In the field of self-assembly, one of the pioneering studies was conducted by Muller’s research group. In 2001, synthetic “Janus micelles” were first synthesised by Müller using self-assembly technology. His approach of solution-casting–cross-linking–redissolution was relatively simple and laid the foundation for the

development of self-assembly technology.<sup>96</sup> Thus, a wide variety of Janus particles can be synthesised in a controlled manner *via* self-assembly.<sup>3,97,98</sup> Recently, some “subtractive” methods have been proposed. UV-etching is considered one of the best “subtractive” methods because of its versatility and environmental friendliness. Recently, Chen’s research group has made a series of advances in the synthesis of Janus NPs by UV cleavage.<sup>99–101</sup> In 2021, they proposed a simpler two-step synthetic method for preparing Janus NPs. They first synthesised a particle film at the gas–solid interface and then placed the film directly under an ultraviolet light source for photodegradation. In a short time, they achieved a coverage rate of 43.49% in the film.<sup>102</sup> However, the subtractive method is currently not mature enough, and further studies are encouraged to achieve a high-yield synthesis of Janus particles of interest.

### 3.4 Molecular precision surface engineering by bottom-up synthesis

**3.4.1 DNA nanotechnology-based surface decoration.** DNA is an effective programming material with good addressability, controllability, and biocompatibility. Based on the Watson–Crick complementary base-pairing principle, DNA is constructed into various nanomaterials (from tiles to origami), which are expected to play a role in drug delivery and computer programming.<sup>103,104</sup> However, the relatively simple physical and chemical properties limit the application of DNA nanostructures. Therefore, many nanotechnology-based surface modification methods have been proposed to solve these problems. Origami, synthesized by hundreds of strands *via* a one-pot method, shows an unprecedented ability for precisely attaching the ligand, where the strand can be extended as an anchor for any further modifications.<sup>105</sup> Based on that, Ke *et al.* showed that it is easy to precisely combine a nucleotide probe to an anchor strand *via* specific base pair recognition. Moreover, the following probe–target binding affinity is related to the probe’s position on origami—the edge position results in the best efficiency, while the middle position results in the worst.<sup>106</sup> Similarly, a common method to attach other groups (*e.g.* proteins) is to conjugate the group of interest to an oligonucleotide, followed by its hybridization.<sup>107,108</sup> Moreover, the origami-mediated assembly of carbon nanotubes in high resolution provides a paradigm to produce the desired complex pattern.<sup>109</sup> To further prove their functionality, in 2010, Voigt *et al.* demonstrated their viability as locally addressable solid supports for post-assembled precise modifications. In their research, strands with various groups were distributed, respectively, at the correct position before undergoing cleavage and coupling reactions without crosstalk.<sup>110</sup> As a result of these decoration methods, polymers can be added to origami through electrostatic interactions, hydrogen bonds or hydrophobic forces, and nucleic acid hybridisation. This polymer-origami method is a good tool for nanostructure construction.<sup>111,112</sup> For example, the addition of hydrophobic molecules to origami facilitates the construction of amphiphilic DNA nanostructures. In 2014, the Liu group added aryl ether and ethylene glycol to the staples and then combined these

staples with origami to form a self-folding amphiphilic origami.<sup>113</sup> Subsequently, in 2016, they constructed a 2D amphiphilic nano-molecular layer in a controlled and independent manner (Fig. 2a).<sup>114</sup> A key goal of researchers is to incorporate DNA nanostructures into organisms. Because of the hydrophobic force between the cholesterol moieties on the DNA nanostructures and the lipid membrane, the construction of switchable DNA nanostructures attached to the lipid membrane is very simple.<sup>115,116</sup> To highlight this, researchers have successfully constructed simulated molecular channels on the lipid membrane using DNA nanostructures.<sup>13</sup> In addition, Li *et al.* used tubular origami-coated thrombin and nucleic acid aptamers as targeting ligands to achieve thrombosis at targeted cancer sites, providing a new methodology for the hypoxia treatment of cancer (Fig. 2b).<sup>117</sup> This process heavily relies on the precise linkage of lockers on DNA origami to ensure the appropriate transition from a ‘closed’ state to an ‘open’ state. Moreover, DNA origami serves as a perfect platform for the construction of a molecular robot. As researchers can attach strands on origami in an approximately 6 nm resolution, robots can accurately go through the path, thus performing the desired function.<sup>118,119</sup> Among them, a cargo-sorting robot has been constructed by Thubagere, showing the intelligence of a DNA nanorobot.<sup>120</sup>

**3.4.2 Protein nanostructure-based surface engineering.** Compared to the DNA nanomaterials mentioned above, proteins can be considered “natural nanoparticles”. Due to their low toxicity, protein-based nanostructures are more advantageous for use in organisms (Fig. 2c).<sup>121</sup> Moreover, because of its isotropy, a single product can be easily obtained from the capsid.<sup>122</sup> Most importantly, a virus capsid can undergo surface engineering at a specific site *via* genetic or chemical modifications. Therefore, surface engineering has been employed to modify virus nanostructures for application in various fields (Fig. 2d).<sup>123</sup>

Adenovirus (Ad) is the most frequently used gene transfer vector in clinical trials, and to achieve its clinical applications, various methods have been proposed. There are mainly three biological (genetic) methods to engineer its surface pattern. (1) Insertion of antigenic epitopes in the adenovirus fibre protein is mainly realized by adding targeting ligands to an adenovirus fibre knob, for example, RGD modified adenovirus can bind to integrin.<sup>124</sup> In 2015, Hanni succeeded in attaching the epidermal growth factor to the epidermal growth factor receptor for circumventing pre-existing Ad5 immunity in clinical populations.<sup>125</sup> (2) The second method is switching the serotype of adenovirus, such as transforming the fibre portion of Ad5 into that of Ad6/Ad35.<sup>126,127</sup> (3) The third method is the removal of the liver targeting fibre protein. In this method, Ad can be more biocompatible. For example, Leissner *et al.* artificially enabled the mutation of an AB loop(S408E) on Ad5, which then lost its ability to bind to cellular receptors.<sup>128</sup> Moreover, the mutation of the KKTK motif to GAGA can lead to its inability to bind heparan sulphate proteoglycan.<sup>129</sup>

Predominantly, there are three methods to chemically engineer the virus surface pattern. (1) Similar to gene modification,

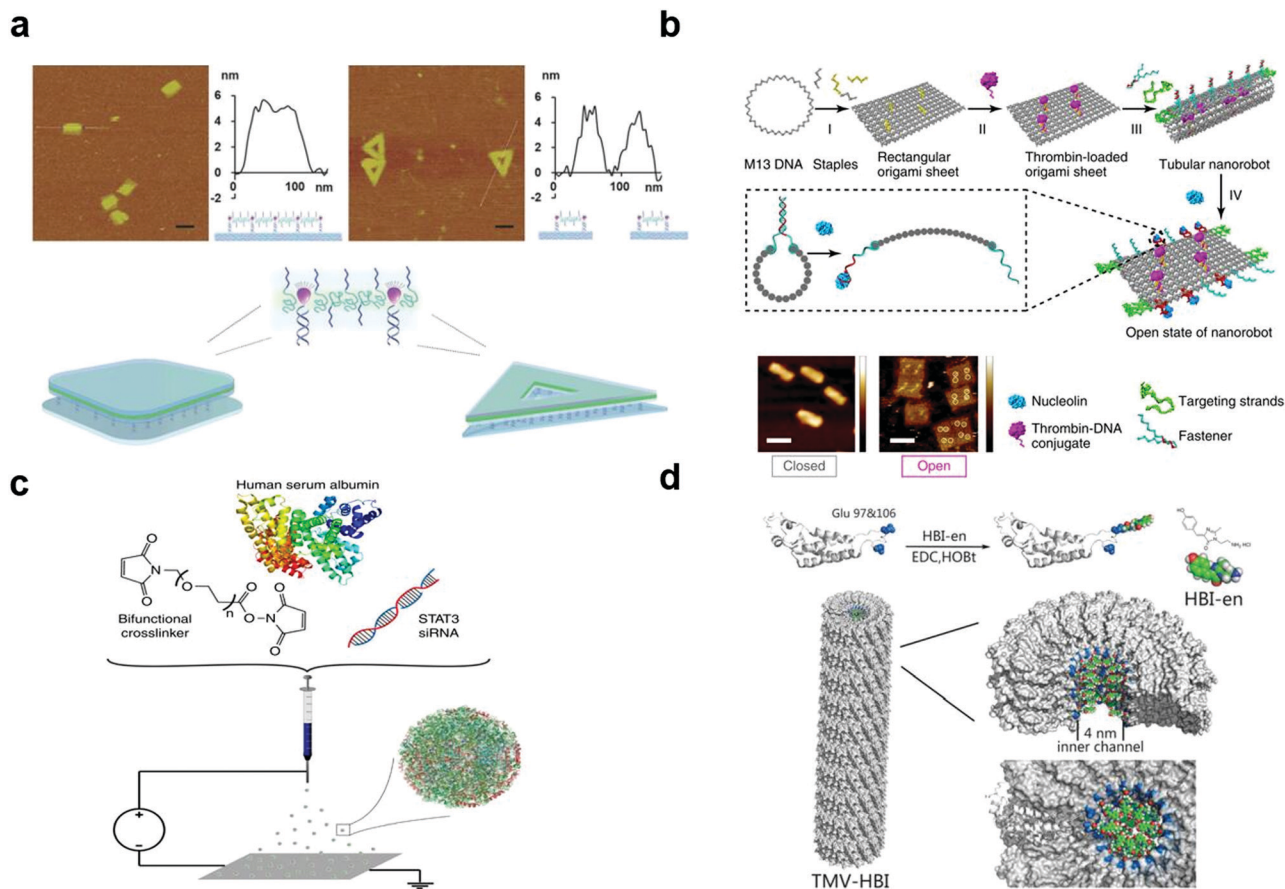


Fig. 2 (a) Illustration of the 2D assembly of amphiphilic molecules *via* a frame-guided process. (b) Scheme of the construction of the DNA origami attached by thrombin. (c) Schematic illustration of the jetting formulation for crosslinked, STAT3i-loaded, iRGD-conjugated, targeted albumin NPs (STAT3iSPNPs). (d) Coupling of HBI-en chromophore and TMV capsid protein with glutamate residues 97 and 106 emphasized (blue). Reproduced with permission from ref. 114, 117, 121 and 123, copyright (2018) Springer Nature, (1996) The Royal Society of Chemistry, (2020) Wiley Online Library and (2020) Springer Nature.

attaching polymers with ligands chemically contributes to the specific function of adenovirus (*e.g.* through interactions with the target tumour tissues).<sup>130,131</sup> (2) Conjugation of positive polymers or lipids is a common way to promote adenovirus entry into a membrane. Given the increased electrostatic interactions, the internalization process does not rely on the mediation of a cellular receptor.<sup>132,133</sup> (3) As different parts of an organism have unique circumstances, it is also our goal to develop virus-based nanoparticles that can respond to specific surroundings. Considering the relatively acidic microenvironment in tumour tissues, hybridization with pH-responsive polymers enables controllable release only at the tumour site.<sup>134,135</sup>

### 3.5 Techniques for the characterization of the nanoparticle surface

To further investigate the surface properties of nanoparticles and to broaden the application prospects of nanoparticles, techniques are needed to characterize the surface patterns on nanoparticles. The attachment of ligands to nanoparticles and the interaction between the whole nanoparticles and their

targets are the focus of the nanoparticle field. Some basic methods have been attempted to roughly characterize the surface of nanoparticles. BET (Brunauer–Emmett–Teller) techniques involve a type of gas absorption experiment and have been employed for the characterization of surface area and porosity, indicating the type of biomolecular interaction that follows (*e.g.* a high surface area and porosity tend to form a protein corona).<sup>136</sup> Zeta potential and electrophoretic mobility can provide basic information on the electrical properties of the nanoparticle surface, but they cannot be used to characterize their microscopic charge distribution.<sup>137</sup> Nuclear magnetic resonance (NMR) spectroscopy serves as a general tool to characterize ligand density and ligand structures, although it is limited by its sensitivity (Table 1).<sup>138</sup>

To provide more detailed information about surface patterns, electron microscopy and atomic force microscopy (AFM) are the main methods proposed thus far. Previous studies have used electron microscopy (transmission electron microscopy) or scanning electron microscopy to elaborately characterize the morphology and growth kinetics of nanoparticles.<sup>139,140</sup> AFM, based on the interaction between the probe and the sample,

Table 1 Techniques for the characterization of the nanoparticle surface

Surface characterization techniques	Usage	Advantages	Disadvantages
BET	Surface area	Rapid and simple	Provides relatively rough information
Zeta potential	Electrical properties	Can partially determine the stability of NPs	Cannot provide the detailed charge distribution
NMR	Properties of ligands	Relatively comprehensive methods to characterize NPs	Low sensitivity, not suitable for metal NPs which induce changes in local magnetic fields
IR methods	Properties of ligands	High sensitivity, merely no restriction on the types of NPs	Qualitative, not quantitative
MALDI-TOF	Properties of ligands	Rapid, sensitive, low cost	Mainly used on protein (peptide) related structures
AFM/SEM/TEM	Size, shape and morphology	Visualized information, very sensitive	Expensive and laborious
HPLC/MS	Linkages between NPs and ligands	Qualitative methods to determine chemical compositions	Involves additional procedures
MD	Folded structures of dendrimers	Accurate when combined with other characterization methods	High computational cost

can also directly provide visualized information about nanoparticles.<sup>141</sup> These methods have been widely used in studies about origami, dendrimers, *etc.* to confirm the correct formation of substructures.

In addition, to further characterize surface patterns, infrared techniques with a high sensitivity have been recognized as versatile methods to study the functional groups on nanoparticles. For example, IRRAS (infrared reflection absorption spectroscopy) analyses thin films mainly by a combination of transmission and reflection IR spectroscopy in a mixed mode to achieve high resolution,<sup>142</sup> although IR based methods are mainly qualitative not quantitative. Furthermore, elemental analysis can provide information on the elemental composition of surface ligands.<sup>143</sup> HPLC/MS (high-performance liquid chromatography/mass spectrometry) can quantitatively characterize the number of nanoparticle surface linkages, which requires some additional procedures before to break the linkages (*e.g.*, Au-S breakage by iodine cleavage).<sup>144</sup> As dendrimers are highly branched, MD (molecular dynamics) simulation has been utilized to analyse these complex structures. It can determine the spatial array of branch points and the molecular surface area; what is more, it can provide more convincing results about these complex highly folded conformations when combined with SAXS (small angle X-ray scattering).<sup>145</sup> In addition, matrix-assisted laser desorption/ionization time-of-flight (MALDI-TOF) mass spectroscopy has been widely applied to assess the ligand labelling efficiency to a virus capsid.<sup>146</sup> Moreover, its analysis is based on the comparison between its mass spectrum and the reference in the database.

## 4. Surface patterns of nanoparticles affect their interaction with the cell membrane

### 4.1 Structure of the cell membrane: mesoscale domain organization of the plasma membrane

The cell membrane is composed of lipids, proteins, and sugars, which constitute the outermost layer of the cell.<sup>21</sup> The cell membrane plays an important role in maintaining cell stability,

energy conversion, information transmission, and material transportation. The study of cell membranes has a long history. Among the studies, the membrane fluid mosaic model proposed by Singer and Nicholson in 1972 was supported by ample experimental evidence and has greatly impacted our understanding of cell membranes.<sup>147</sup> With the development of experimental technology and in-depth research, researchers have found that not all membrane proteins on the cell membrane are free to move. A large number of facts and experimental results<sup>17,148</sup> have proved that the diffusion phenomena of membrane molecules such as transmembrane (TM) proteins, glycosylphosphatidylinositol (GPI)-anchored proteins, and phospholipids are dependent on the regional features, time scale, and actin-base membrane skeleton interaction. This phenomenon is known as hop diffusion.<sup>23,149</sup> Based on these features of hop diffusion, researchers have proposed the anchored membrane protein picket model (Fig. 3a and b).<sup>18,35</sup> In this model, TM actin-binding proteins were aligned along the membrane skeleton and anchored by underlying cortical actin (CA) filaments, thus forming fences, or pickets, which could effectively block the diffusion of relevant membrane molecules.

The cytoplasmic membrane may be divided into three levels on the mesoscale: membrane compartment, raft domain, and protein cluster.<sup>150</sup> The mesoscale is larger than the nanoscale and smaller than the microscale. On this scale, the dynamic processes and interactions of domains or molecules at different levels in space and time can be considered, and the important roles played by thermal fluctuations and weak synergy can be included. Based on this, we will introduce the main contents of the mesoscale domains of the plasma membrane in this section.

The formation of membrane compartments<sup>151,152</sup> occurred because TM proteins were immobilised on the membrane backbone by an interaction with the filamentous actin fence and then formed fences, or pickets, to partition the cytoplasmic membrane into multiple regions (*i.e.*, membrane compartment) (Fig. 3a and b). The membrane compartment has played an important role in promoting the formation of protein complexes on the membrane surface, the distribution and



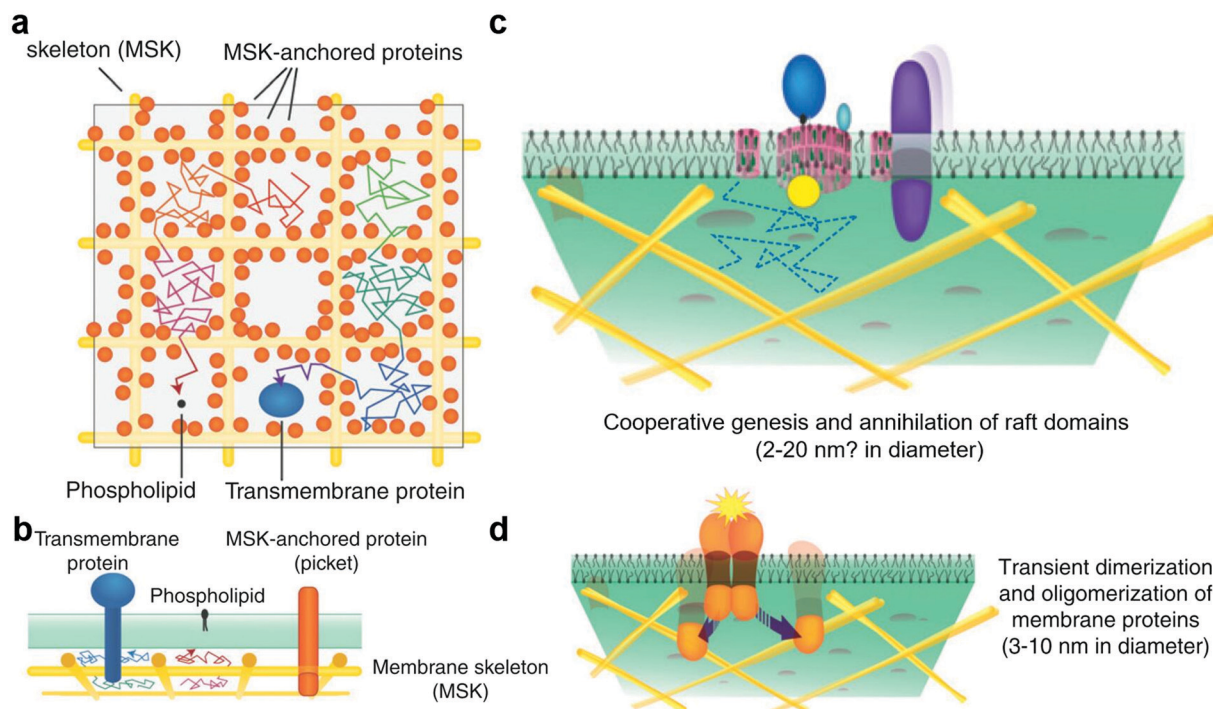


**Fig. 3** (a) Top view of the anchored membrane protein picket model and membrane compartment. (b) Side view of the anchored membrane protein picket model and membrane compartment. (c) In the raft domain, the size of cholesterol is limited by the membrane compartment. (d) Protein clusters form on the membrane and then disaggregate. Reproduced with permission from ref. 17, copyright (2011) Elsevier.

diffusion of different membrane molecules on the membrane surface, and the size limitation of the raft domain. These effects cannot be separated from the existence of proteins, such as TM proteins, and their molecular interactions.

The raft domain<sup>19,22,153</sup> is a nano-scale, heterogeneous, highly dynamic, and relatively ordered membrane domain rich in sterols and phospholipids (Fig. 3c). The formation, size, and existence time of the raft domain are affected by intermolecular affinity and thermal fluctuations. The molecules that affect raft formation include lipids and proteins. Lipid interactions based on cholesterol and saturated acyl chains recruit molecules that gradually form dynamic transient raft complexes. The membrane compartment also plays an important role in the size of the raft domain. The raft domain plays an important role in cell signal transduction, transmembrane transport of substances, and invasion by pathogenic microorganisms. The realisation of these functions may be closely related to the assembly and size regulation of a raft.

Protein clusters are dimers or oligomers of proteins or more complex and large protein complexes (Fig. 3d).<sup>154–156</sup> These protein complex domains play an important role in cell signal transduction, transmembrane transport of substances, and other functions. The membrane compartment plays an important role in promoting the formation of protein clusters, such as protein dimers. In the cell signal transduction function, protein complex domains can synergistically assemble cholesterol and saturated lipids to form a raft and form a synergistic complex after binding to related molecules to exert related

functions. This synergistic effect is of great significance for the protein to exert its function or for enzyme activity.

The three hierarchical structures on the cell membranes of organisms have dynamic relationships. The cell membrane is a complex system, which is affected not only by the cell surface molecules, but also by the intracellular and extracellular environments. The following sections will introduce how nanoparticles with hydrophobic and hydrophilic surface patterns interact with the cytoplasmic membranes as well as the basic mechanisms and processes involved, which are inseparable from the basic characteristics of the cell membrane and the surface characteristics of nanoparticles.

## 4.2 Fine-tuning of surface hydrophobicity and charge patterns for membrane interaction

### 4.2.1 How surface hydrophobicity and charges influence the interaction between nanoparticles and membranes.

Surface hydrophobicity and charges are the most critical surface properties affecting nanoparticle interactions with the cell membrane. Many experiments prove that tuning the hydrophilic and hydrophobic structures could efficiently regulate the transport of nanoparticles into cells. Castro *et al.* reported that poly(ethylene oxide)-*b*-poly( $\epsilon$ -caprolactone) nanoparticles with a higher level of hydrophobicity could be transported across the membrane more efficiently than poly(ethyleneoxide)-*b*-poly(lactic acid) nanoparticles in the cell uptake experiment with the human glioblastoma cell line U251.<sup>157</sup> By linking the hydrophobic ligand octanol to glutathione-coated AuNPs

(OG-AuNPs), the hydrophobicity of AuNPs could significantly enhance their affinity for the cell membrane.<sup>158</sup> Guo *et al.* demonstrated the direct transport of nanoparticles covered with hydrophobic lipids.<sup>159</sup> They used fluorescent lipids to study the spontaneous formation of pores by AuNPs on the membrane and the occurrence of lipid exchange. This mechanism may explain why nanoparticles can spontaneously penetrate the membrane and enter the cell but cannot escape from the cell, which also revealed that the local hydrophilicity of particles plays a key role in the interaction with the cell membrane, resulting in different rollover and movement behaviors of particles in the cell membrane.

However, in addition to considering the positive effect of hydrophobicity on the cellular uptake of nanoparticles, we should also note the negative effect of surface hydrophobic groups on the adsorption of proteins in organisms and the nonspecific aggregation during circulation.<sup>160,161</sup> Therefore, the balance between the hydrophobic and hydrophilic surfaces of nanoparticles plays a very important role in the complete functional path of nanoparticles, such as transportation, ingestion, and drug release in organisms, which deserves further research. This can help researchers design more reasonable and effective nanocarriers, opening up a way to solve practical problems.

From this aspect, nanoparticles with patterned hydrophobic and hydrophilic surfaces should be more preferred to benefit from the hydrophobic interactions with the membrane and also compensate the disadvantages. In recent years, computer simulation has already shown the internalization process and mechanism of nanoparticles with different surface patterns. Li *et al.* compared striated nanoparticles with hydrophilic and hydrophobic ligands alternately arranged at intervals, fully hydrophilic nanoparticles, fully hydrophobic nanoparticles, and NPs with randomly mixed ligands at the same hydrophilic to hydrophobic ratio.<sup>161</sup> They found that striated nanoparticles had the lowest energy barrier and were easy to transport. Through a dissipative particle dynamics (DPD) simulation, they verified the existence of a new type of amphiphilic nanoparticle–ligand complex that spontaneously penetrates the cell membrane.<sup>162</sup> Notably, there are also significant differences in the interaction between nanoparticles with different patterns and cell membranes, such as stripes, a random distribution, and other patterns. Zhang *et al.* simulated four kinds of copolymer-coated nanoparticle complexes (including hydrophilic–hydrophobic (AB), hydrophobic–hydrophilic (BA), hydrophobic–hydrophilic–hydrophobic–hydrophilic (BABA), and random hydrophilic–hydrophobic patterns with different characteristics) by using dissipative particle dynamics to explore the effects of the density, rigidity, and surface pattern on the nanoparticle surfaces during their transport through the cell membrane. They found that BA and BABA patterns play important roles in the transport process.<sup>163</sup>

Except from hydrophobicity, the surface charge distribution of nanoparticles is also essential in the controlled transport process, and the charge plays an important role in the interaction between nanoparticles and the phospholipid

membrane.<sup>5,164</sup> For instance, negatively charged AuNPs are not easily fused with cell membranes because they are repelled by electrostatic interactions with the negatively charged cell membranes.<sup>165,166</sup> At the same time, positively charged AuNPs usually have high cell membrane permeability. Goodman *et al.* reported that the cytotoxicity of positively charged AuNPs was much higher than that of negatively charged AuNPs, and this result is likely to be related to their different cellular uptakes.<sup>167,168</sup> Ma *et al.* fabricated different kinds of chitosan-based nanoparticles, which could carry different charges but were identical in other characteristics (the size, shape and hydrophobicity). They incubated these nanoparticles with different cell lines to uncover the biological effects of nanoparticles. The experimental results indicated that positively charged nanoparticles would promote the transmembrane efficiency of nanoparticles. They also observed different intracellular trafficking effects induced by different charged surfaces of nanoparticles.<sup>169</sup>

These studies strongly supported the importance of constructing hydrophobic patterns and charge structures on nanoparticles for cell interactions. However, the experimental proof of this concept is still challenging. Only dendrimers and AuNPs have been successfully constructed with defined surface hydrophobicity and charge patterns and investigated their influence with cells. Therefore, the following two sections will introduce both systems in detail.

#### 4.2.2 Interactions between dendrimers and membranes.

Because of their versatility, flexibility, and modifiability, dendrimers have broad prospects in the field of drug delivery and nucleic acid delivery. It has long been desired to obtain dendrimers that are structurally stable, have low toxicity, and can be efficiently taken up by cells. Many studies have demonstrated the important effects of surface characteristics, size, and other related factors on the uptake of nanoparticles by cells.<sup>170</sup> There is a general understanding that positively charged dendrimers, such as poly(amidoamine) (PAMAM) dendrimers, could more efficiently penetrate cell membranes. Computer simulations also illustrated the detailed process of how PAMAM dendrimers interact with cell membranes. However, large-sized PAMAM molecules with high positive charges can cause the formation of pores on the cell membrane and even cell death (Fig. 4a and b).<sup>171–176</sup> This greatly limits the application and development of related dendrimers.

By designing proper surface patterns, one could also achieve efficient cell uptake similar to PAMAM but without a high density of positive charges. In the previous section, we introduced the methods to create polyphenylene dendrimers (PPDs) with defined surface patterns. These dendrimers are highly branched, shape durable, and monodisperse. In addition, they can be chemically functionalized at their core, scaffold, and surface, which provides the possibility of regulating the surface characteristics of PPD. Therefore, they are one of the successful models that are used to study the effect of surface patterns on cell interactions.

Müllen and Weil *et al.* made important contributions to the biological applications of PPDs. In their work in 2014, they

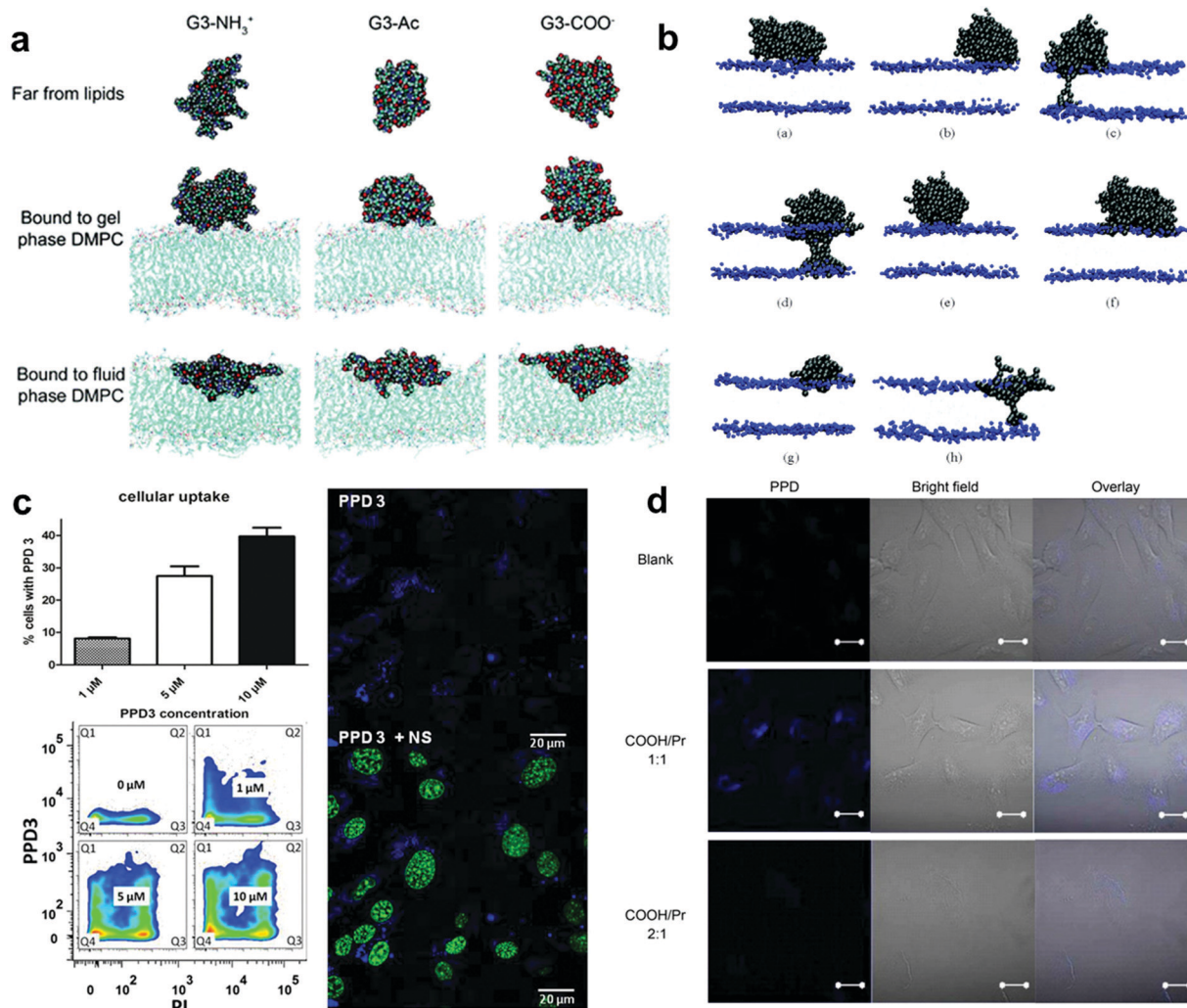


Fig. 4 (a) Representative images of G3 with different terminations of the dendrimer in different equilibrated states. (b) Snapshots of different simulations of systems with different dendrimers. (c) PPD3 uptake and influence on brain endothelial cells. (d) Confocal fluorescence images of HLC cells incubated for 24 h with PPD. Reproduced with permission from ref. 173, 176, 91 and 178, copyright (2009) MDPI, (2006) American Chemical Society and (2014), (2017) Wiley Online Library.

demonstrated that PPDs with design alternating hydrophobic and hydrophilic patterns could display similar performance to the natural proteins, demonstrating their biocompatibility and application potential.<sup>91</sup> Instead of using positive charges to enhance membrane interactions, the negatively charged hydrophilic groups were adopted in their systems which are normally not preferred for cell uptake. Surprisingly, by optimising the hydrophilic and hydrophobic patterns on the surface, these PPDs could be efficiently taken up by cells and even able to penetrate blood brain barrier models without affecting the membrane integrity.<sup>177</sup> PPDs form 3D spheroids in aqueous solution with lipophilic cavities inside (like a protein structure). Researchers assigned the molecule a biological identity similar to that of human serum albumin (HSA), a natural vehicle for transporting lipophilic or poorly water-soluble substances with abundant animal plasma. The characteristics of this new PPD can be summarised as follows: (1) nanometer size, (2) a spherical structure with an amphiphilic surface pattern that

promotes the interaction with the cell membrane, and (3) lipophilic internal cavities with different nanoscale dimensions that provide controllable guest uptake. PPDs exhibited good transport in A549 cancer cells and endogenous brain cells and low toxicity in relevant experiments. These results strongly supported that tuning the patterned structures on the nanoparticle surface could be an efficient way to promote cell interactions (Fig. 4c).

In another study, they performed surface tension measurements, X-ray reflex (XR), and sum-frequency generation spectroscopy (SFG) to study the effect of charges of the hydrophilic groups on amphiphilic PPDs (approximately 5 nm in diameter) using the monolayer of a self-assembled cell membrane (1,2-dipalmitoyl-*sn*-glycero-3-phosphocholine [DPPC]).<sup>8</sup> This work showed that the dendrimer interacted with the cell membrane *via* the electrostatic force of the lipid headgroup, which drove the changes in headgroup alignment, and the negatively charged dendrimer could induce behavioural changes in



interface water molecules. The results of this study have deepened the understanding of the interaction between amphiphilic PPD macromolecules and the lipid layer and improved its application in biology.

In their work in 2017, Müllen *et al.* demonstrated how the type and ratio of hydrophilic groups on amphiphilic PPDs influence the interaction with biological systems and studied their manifestations in cellular uptake and toxicity (Fig. 4d).<sup>178</sup> A PPD with a molar ratio of propyl groups to sulfonic acid (*i.e.* non-polar to polar groups) of 1:1 as the surface feature was used as the parent molecule, and weakly acidic carboxylic or phosphonic groups were used to replace the surface sulfonic acid to explore the effects of acidic changes and the ratio of polarity to non-polarity on the surface of the dendrimer to explore the important effects of the PPD surface-patched architecture on the uptake of substance particles by cells. Different groups had little effect on substance transport and cell uptake. Almost all the dendrimers with a molar ratio of polar to non-polar groups of 1:1 showed high cell uptake, while the dendrimers with a molar ratio of polar to non-polar groups of 2:1 could not cross the cell membrane. Researchers believe that this is because the high density of polar groups enhanced the rejection of PPDs against the cell membrane. This result demonstrates the important role of highly hydrophobic (lipophilic) surface features (*i.e.*, high coverage of hydrophobic groups) in promoting cell uptake. This work is of great significance for the future design of feasible vectors for patched PPD-related drugs and nucleic acids.

Overall, these studies supported that the hydrophobic and hydrophilic surface patterns could significantly influence the interactions with cell membranes, and particularly the type of hydrophilic groups, hydrophobic groups and their ratio are all essential to tune the interactions. In this regard, the highly branched, shape-persistent, monodisperse PPDs with precisely designable surface patterns and special internal cavity structures offer the possibility and feasibility of their interaction with biological systems and their subsequent applications.

**4.2.3 Interaction of AuNPs with membranes.** The surface hydrophobicity, hydrophilicity, and charges on AuNPs play an important role in cell uptake and nanoparticle–cell membrane interactions.<sup>179,180</sup> Understanding the interaction between AuNPs and the membrane system and the related influencing factors is of great significance for their biomedical applications. Okoampah *et al.* have systematically summarized the influences of different factors on the interaction between gold nanoparticles and the cell membrane.<sup>181</sup> At present, it is believed that the transport pathways of AuNPs are mainly the endocytosis pathway and direct penetration.<sup>182,183</sup> There are also differences in the internalization pathways of gold nanoparticles of different sizes (Fig. 5a and b).<sup>184,185</sup> The surface pattern and related functional groups, as well as the characteristics, proportions, distributions, and structures, of the ligands have an important impact on the biological behaviour of AuNPs. Quan *et al.* explored the interaction between AuNPs with different surface characteristics and asymmetric lipid membranes by using coarse-grained molecular dynamics

(CGMD) simulations, revealing the mechanism of interaction between nanoparticles and asymmetric lipid membranes to a certain extent (Fig. 5c).<sup>164</sup> Researchers can even control and design the behaviour and whereabouts of AuNPs based on the regulation and control of the surface pattern.

With the methods discussed in Section 3.1, it is possible to create fine substructures on the surface of AuNPs and thus investigate their effect on membrane interactions in more detail. Recently, Lunnoo *et al.* theoretically demonstrated that, compared with AuNPs with pure positive/negative charges, zwitterionic particles are less likely to be inside the membrane due to the rise of free energy barrier. In addition, zwitterionic particles prefer to agglomerate, which can further reduce its translocation rate.<sup>186</sup> However, as mentioned above, zwitterionic modification can prevent the arbitrary absorbance of these macromolecules, and delicate distribution of these 2 opposite ligands is needed to make a trade-off to overcome the dilemma. Moreover, surface electrical density is also viewed as a co-factor in determining the pathway of the particles into the membrane, which implies that it is essential to control the density of charges for avoiding damage to the membrane.<sup>187</sup> This study indicated the promising potential of creating more defined charge separated patterns for fine-tuning of nanoparticle interactions with cell membranes. However, since the techniques to precisely prepare such nanoparticles are still unavailable, this direction remains unexplored.

However, hydrophobic patterns have been created on the AuNP surface which has been shown to strongly influence their interaction with the cell membrane or other biological interfaces. Stellacci *et al.* have made important contributions to the field. In their early work, they reported related research on AuNPs covered with hydrophobic ligands (octanethiol, OT) and hydrophilic ligands (mercaptopropionic acid, MPA). They found that the self-assembly of AuNPs formed a striped structure, and the transmembrane transport of this particle in fibroblast cells was also observed.<sup>188,189</sup> The results from the Stellacci group revealed the potential of nanoparticle surface patterns in regulating the material internalisation mechanism. Gkeka *et al.* extended the work of Stellacci *et al.* to explain the mechanism of regular surface patterns promoting transport to some extent by coarse-grained molecular dynamics simulations. Designing nanoparticles with a certain amphiphilic pattern on the surface may be an excellent application scheme.<sup>190</sup>

The above studies demonstrate that the design of more sophisticated structures (the heterogeneous surfaces) can obtain finer particles. Gao *et al.* studied the possible effects of hydrophilic and hydrophobic structures of nanoparticles on transmembrane behavior *via* computer simulations. Homogenous hydrophilic particles can only be absorbed on the membrane surface rather than enter the lipotropy phospholipid bilayer. However, for homogenous lipophilic nanoparticles, it may be easier to be inserted inside the lipotropy phospholipid bilayer, but more difficult to be released. Homogenous lipophilic nanoparticles could even cause substantial disruption to the bilayer while leaving the membrane.<sup>191,192</sup> Due to



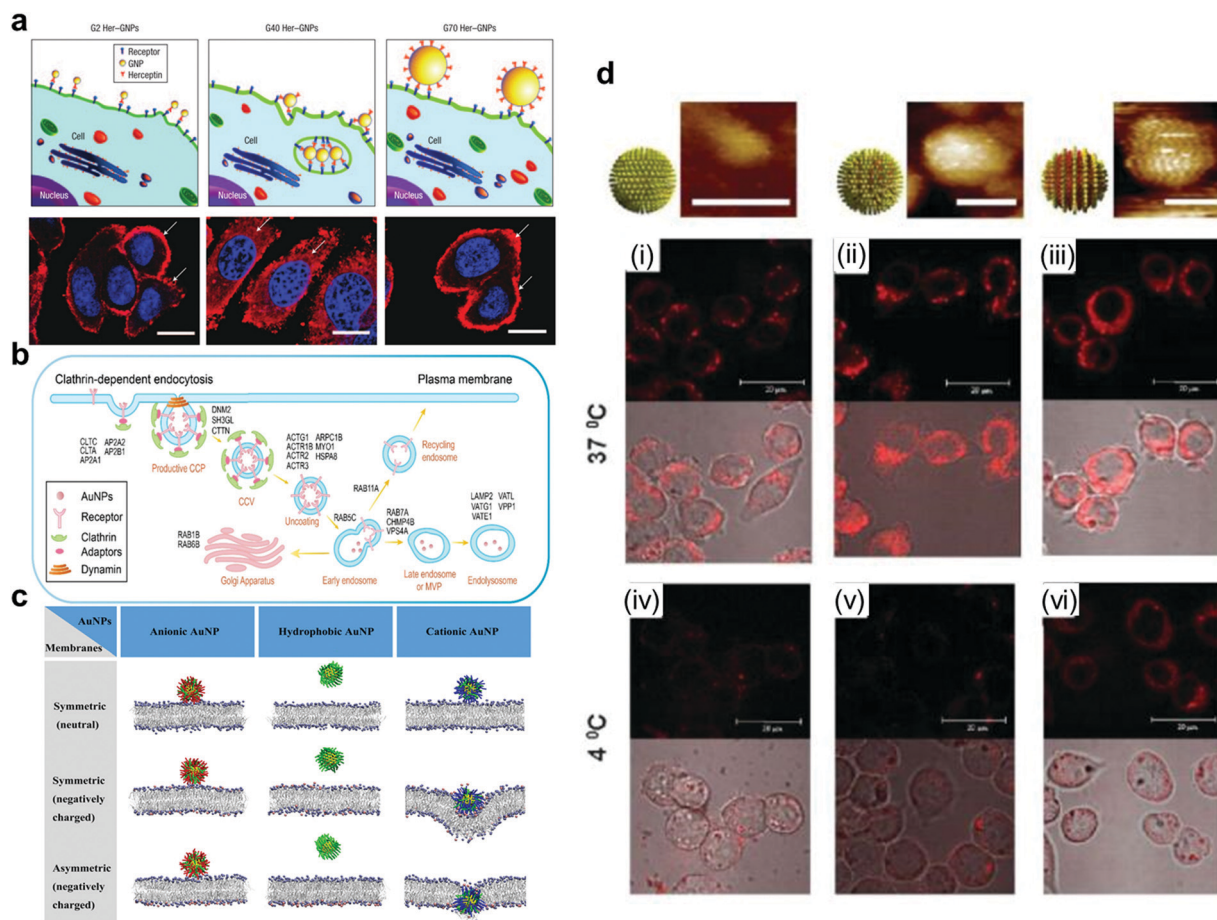


**Fig. 5** (a) Fluorescence image of ErbB2 receptor localization after treatment with different sizes of Her-GNPs. (b) Illustration of AuNPs internalized by the cell in a receptor-mediated manner. (c) AuNPs with different charges interact with symmetric or asymmetric lipid membranes. (d) AuNPs with different structural organizations of hydrophilic and hydrophobic ligands on the surface display different transmembrane abilities and phenomena when interacting with the cell membrane. Reproduced with permission from ref. 164, 184, 185 and 189, copyright (2008) Springer Nature, (2021) American Chemical Society, (2020) Elsevier and (2010) Wiley Online Library

the amphiphilic characteristics of the phospholipid bilayer, AuNPs with amphiphilic patterns are more likely to interact with cell membranes and thus have higher cell uptake efficiency. Stellacci and Alexander-Katz *et al.* elucidated the mechanisms of spontaneous insertion of amphiphilic AuNPs into the membrane by conducting unbiased atomistic simulations and experimental verification.<sup>193</sup> They demonstrated the vesicle fusion-like and non-disruptive behaviour between amphiphilic AuNPs and the membrane.

The structural organization of hydrophilic and hydrophobic ligands on the AuNP surface also play an important role in the interaction between the nanoparticles and cell membrane. Stellacci *et al.* used hydrophobic and hydrophilic ligands to construct patterns with different structural organization patterns on the particle surface, demonstrating that nanoparticles coated with a ribbon-like alternating arrangement penetrated the cell membrane. However, particles coated with the same ligands but in a random arrangement cannot penetrate the membrane effectively, and can even get trapped in vesicular bodies (Fig. 5d).<sup>189</sup> Therefore, the process of AuNP incorporation is a result of many factors.

### 4.3 Fine-tuning of ligand patterning for receptor mediated cell recognition

**4.3.1 Effect of ligand density on nanoparticles.** In the previous section, we summarised the effects of surface hydrophilicity and hydrophobicity, charge properties, and plaque formation of nanoparticles upon their entry into cells. In addition, the ligand density of nanoparticles is also considered a critical factor in receptor-mediated endocytosis of nanoparticles. One pioneering study was conducted by Adachi, who discovered in 1994 that nanoparticles with a high ligand density were more likely to enter cells than nanoparticles with a low ligand density.<sup>194</sup> The effect of ligand density on multiple receptor-ligand systems was then revealed, and the ligand density of nanoparticles may be positively correlated with the efficiency of their endocytosis to a certain extent.<sup>195</sup> Some early thermodynamic models have been established to explain these phenomena.<sup>196–198</sup> Based on the energy transfer process of receptor-ligand binding (the receptor-mediated adhesion energy surpasses the membrane bending energy), Gao *et al.* analysed the process of spherical nanoparticles and cylindrical

nanoparticles entering cells. They believed that the radius of the nanoparticles was closely related to the ligand density. Based on this model, it could be predicted that the ligand density of the nanoparticles must be greater than a critical value to enter the cells. The range of the radius of the nanoparticles that can be internalised is determined by the two real roots of the equation they proposed.<sup>199</sup>

However, these studies were all based on the ideal state in which all the ligands on the surface of the nanoparticles bind to the receptor in a one-to-one manner. Therefore, in 2010, Yuan considered ligands that did not bind to the receptor and initially established a functional model of nanoparticle ligand density ( $\xi$ ) and endocytosis time. His model is similar to a parabola in that, before the turning point, the greater the density, the shorter the endocytosis time; after the turning point, the greater the density, the longer the endocytosis time. At the turning point, the time is the shortest.<sup>200</sup> Subsequently, Yuan established a more refined 3-phase model. He summarised the optimal nanoparticle endocytosis parameters,  $R$  (radius)  $\in [25, 30]$  nm and  $\xi$  (ligand density)  $\in [0.8, 1]$ , which promoted the design of nanoparticles and their application in organisms.<sup>201,202</sup>

In addition to these simulations, some cellular experiments have demonstrated the effects of nanoparticle ligand density. The mode of endocytosis of folic acid-modified QDs in HeLa cells was closely related to the density of folic acid. When the density ranged from low to high, the endocytosis mode changed from caveolin-mediated to mixed type and finally to clathrin-mediated.<sup>203</sup> Similarly, in 2020, Marine found that the density of the C-type lectin-like molecule-1 binding peptide (cCBP) on the nanoparticle surface determines its way into cells; at a high ligand density, the particle was internalised through the C-type lectin-like molecule-1 (CCL1) receptor, and at a low ligand density it was internalised through the membrane *via* a non-receptor pathway.<sup>204</sup> To better regulate the interaction between nanoparticles and cells, more studies are needed to explore the effect of ligand density on the mechanism of nanoparticle entry into cells.

**4.3.2 Effect of ligand position on nanoparticles.** In addition to the ligand density of the nanoparticles, the distribution of ligands on the surface of the nanoparticles may also be an important factor affecting the endocytosis of the nanoparticles by cells in a receptor-mediated manner. In nature, viruses can enter cells through receptor-mediated endocytosis, leading to gene replication and protein synthesis. On the surface of the nanosized virus capsid, the spike is uniformly distributed.<sup>205</sup> Inspired by this distribution of ligands, some symmetrical nanoparticles have been produced and could be used in organisms for intracellular endocytosis.<sup>206</sup> This homogeneously distributed ligand pattern may facilitate the encapsulation of the entire ligand and allow its subsequent internalisation by the cells.<sup>207</sup> However, whether a uniformly distributed pattern is always the best choice for design under all circumstances remains controversial. The conditions applicable to the uniform distribution of ligands predicted by different models and obtained by cell experiments are inconsistent.

In 2015, Schubertová used a coarse-grained model to characterise the endocytosis process. In his research, the particles

were divided into three categories. For particles with a low ligand density, endocytosis did not occur; for particles with a high ligand density, endocytosis occurred quickly. More importantly, for particles with a medium ligand density, the more symmetrical the ligand distribution, the shorter the endocytosis time. He believed that, for homogeneously distributed nanoparticles, a lower activation energy was required for endocytosis.<sup>208</sup> Subsequently, Li *et al.* considered the mobility of receptors on cell membrane and found the endocytosis rate of nanoparticles was determined by the mutual effect of the distribution of ligands on nanoparticles and the density of receptors on cell membrane. The endocytosis rate of nanoparticles with homogeneously distributed ligands was the fastest only when the density of receptors on the cell membrane was sufficiently high. In most cases, a slightly nonuniform distribution was the best option.<sup>209</sup>

However, in contrast to these two models, Moradi demonstrated that “clustering distribution” enhanced the efficiency of endocytosis compared to “loose distribution”. He examined the phagocytosis of polystyrene nanoparticles with different distribution patterns of folic acid by bronchial epithelial cells and found that the aggregated distribution of nanoparticles exhibited a lower endocytosis efficiency only in the case of a lower folate density.<sup>210</sup> Therefore, cell membrane components (cholesterol, glycoprotein) and intracellular substances (enzymes, reticulin) neglected in previous models might affect receptor-mediated nanoparticle endocytosis.

As mentioned above, DNA origami enables the precise position of ligands, and previously studies have been conducted regarding the influence of the ligand position on receptor-mediated recognition. In 2014, the Teixeira group first demonstrated the feasibility of regulating the receptor function through the nanoscale distribution of ligands (ephrin-A5). They found that the close positioned ligand can promote the recruitment of non-bound receptors (EphA2) and therefore can activate the pathway to a greater extent.<sup>211</sup> Based on this, in 2020, they further found that the located ligands with different interval distances can trigger different downstream transcriptional responses.<sup>212</sup> In addition, the distances between aptamers determine the corresponding cellular behaviours.<sup>213,214</sup> These results demonstrate the importance of accurately positioning ligands to enable them to perform their desired function.

In summary, under all circumstances, the optimal distribution of ligands needs to be fully considered as all of their factors (size, shape, density, and position) are closely correlated. Therefore, a fully established system to elucidate the effects of these factors on the downstream reactions is needed in this field.

## 5. Surface patterns affect protein adsorption

### 5.1 Surface properties of nanoparticles affecting protein corona formation

Because nanoparticles have a high specific surface area, they will interact with the surrounding proteins to produce protein coronas in the biological environment (such as blood and cell

lysates).<sup>215–217</sup> According to the theory of Derjaguin–Landau–Vervé–Overbeek (DLVO), due to the interaction of van der Waals forces with static electricity, biological macromolecules will be spontaneously deposited on the surface of nanoparticles.<sup>218</sup> The nonpolar regions on the surface of the nanoparticles present in the water environment may be more likely to become sites for the binding or adsorption of biological macromolecules.<sup>219</sup>

The formation of a protein corona has a significant impact on the basic characteristics and specific applications of the surface of nanoparticles.<sup>220–222</sup> The formation of a protein corona may also have an important impact on the *in vivo* distribution of nanoparticles, cell uptake mechanisms, the number of nanoparticles ingested,<sup>39,161,223–226</sup> and the cytotoxicity of nanoparticles,<sup>227–231</sup> and even change the function and biological characteristics of nanoparticle targeting.

The compositions of core materials,<sup>232</sup> nano-size,<sup>14,233–235</sup> and surface characteristics<sup>217,219,220</sup> of nanoparticles are of great significance for the formation of a protein corona. Among the various influencing factors, the surface charge and hydrophilic/hydrophobic characteristics of particles play a key role in various biological phenomena.

Many studies on synthetic nanoparticles have shown the possible influence of surface charges on protein–nanoparticle interactions. As the physiological pH is 7.4, many proteins are negatively charged<sup>215</sup> and positively charged nanoparticles may be more likely to interact with them. Boyles *et al.* investigated the interaction between AuNPs with different surface charges (*e.g.* chitosan–AuNP conjugates) and proteins in the cell culture. Their results indicated that surface charges are critical for protein–nanoparticle interactions and their metabolic processes.<sup>236</sup> With the increase of the quantity of surface charges, the positively charged chitosan–AuNPs adsorbed proteins increasingly. Fleischer *et al.* found that, after the bovine serum albumin (BSA) was adsorbed on the surface of the nanoparticles, the interaction between the BSA–NP complex and the cell membrane also changed (Fig. 6a).<sup>237</sup> A summary of the effects of particle surface charge and hydrophobicity on protein adsorption has been presented by some researchers.<sup>217</sup>

The surface hydrophilicity and hydrophobicity of nanoparticles also play a key role in the formation of protein coronas. With an increase in the proportion of hydrophobic groups on the surface, the nanoparticles<sup>238</sup> show a stronger adsorption capacity for substances such as proteins. At the same time, there was a promoting effect on protein corona formation when the number of surface hydrophilic groups was increased. Due to the different types and surface characteristics of nanoparticles and the different biological fluids used for their incubation, there may have been differences in the relationship between the surface hydrophilicity and hydrophobicity of the particles and the formation of protein coronas.

Based on the knowledge about how surface properties influence protein corona formation, it is anticipated that the surface patterns would also play an important role in fine-tuning protein adsorption on nanoparticles. However, studies on this aspect are still limited. Some studies showed that the

use of nanoparticles with amphiphilic surfaces could effectively prevent protein adsorption and protein corona formation in physiological and biological environments.<sup>219,239</sup> Many types of complexes and their effects have been explored.<sup>219,240</sup> However, the understanding of designable surface patterns and their influence on protein adsorption is more challenging. Most studies in this aspect also used the dendrimer and AuNP systems, which will be discussed in detail in the following sections.

## 5.2 Fine-tuning of the surface patterns of AuNPs to control protein adsorption

Because of the high free energy on the surface of AuNPs, AuNPs tend to absorb proteins, thus contributing to the formation of protein coronas.<sup>241,242</sup> After adsorption of some proteins, AuNPs may lose some functions given by artificial modification and may also have new biological characteristics and recognition sites. AuNPs with opsonin or complement proteins can trigger the immune response of biological organisms, which induces their phagocytosis and clearance by macrophages.<sup>39</sup> Therefore, the elucidation of the factors influencing the formation of protein coronas on the surface of AuNPs is essential for their further research and biological applications.

The surface patterns (electrical properties, quantity of electricity and ligand pattern) of AuNPs have an important effect on the formation of various protein coronas with different densities and different components.<sup>243–246</sup>

There exist significant differences in the amount of protein adsorption or composition of a protein corona between particles with different electrical patterns.<sup>247</sup> Nanoparticles with homogeneous charge showed a certain application value in the experiment. However, surface modification with a single electrical structure cannot effectively prevent the protein adsorption. The researchers might be able to achieve better results by constructing zwitterionic surface structures that could increase the biological stability of particles. Researchers have developed various types of zwitterionic surfaces that exhibit good adsorption resistance and biostability.<sup>53</sup> The construction of zwitterionic patterns on the surface of AuNPs can effectively enhance the biocompatibility of nanoparticles and prevent protein adsorption,<sup>248</sup> and this approach has been extensively explored by García *et al.*<sup>249</sup> Gupta *et al.* demonstrated the ability of AuNPs with zwitterions to effectively prevent protein corona formation in serum, improving the colloidal stability of AuNPs (Fig. 6b).<sup>250</sup> Mosquera *et al.* used host–guest interactions to control the zwitterionic surface characteristics of AuNPs with a large size, and this surface property has an important impact on the formation of protein coronas and cellular uptake. Besides, it is noticed that the protein adsorbed on the surface of nanoparticles can be regulated by adding guest molecules instead of the host macromolecular cage to achieve a reversible process (Fig. 6c).<sup>251</sup>

Protein coronas bring many limitations to the practical application of AuNPs, such as cytotoxicity,<sup>252</sup> biodistribution and cellular uptake of AuNPs. Various substances and methods have been tried to prevent the formation of protein coronas by



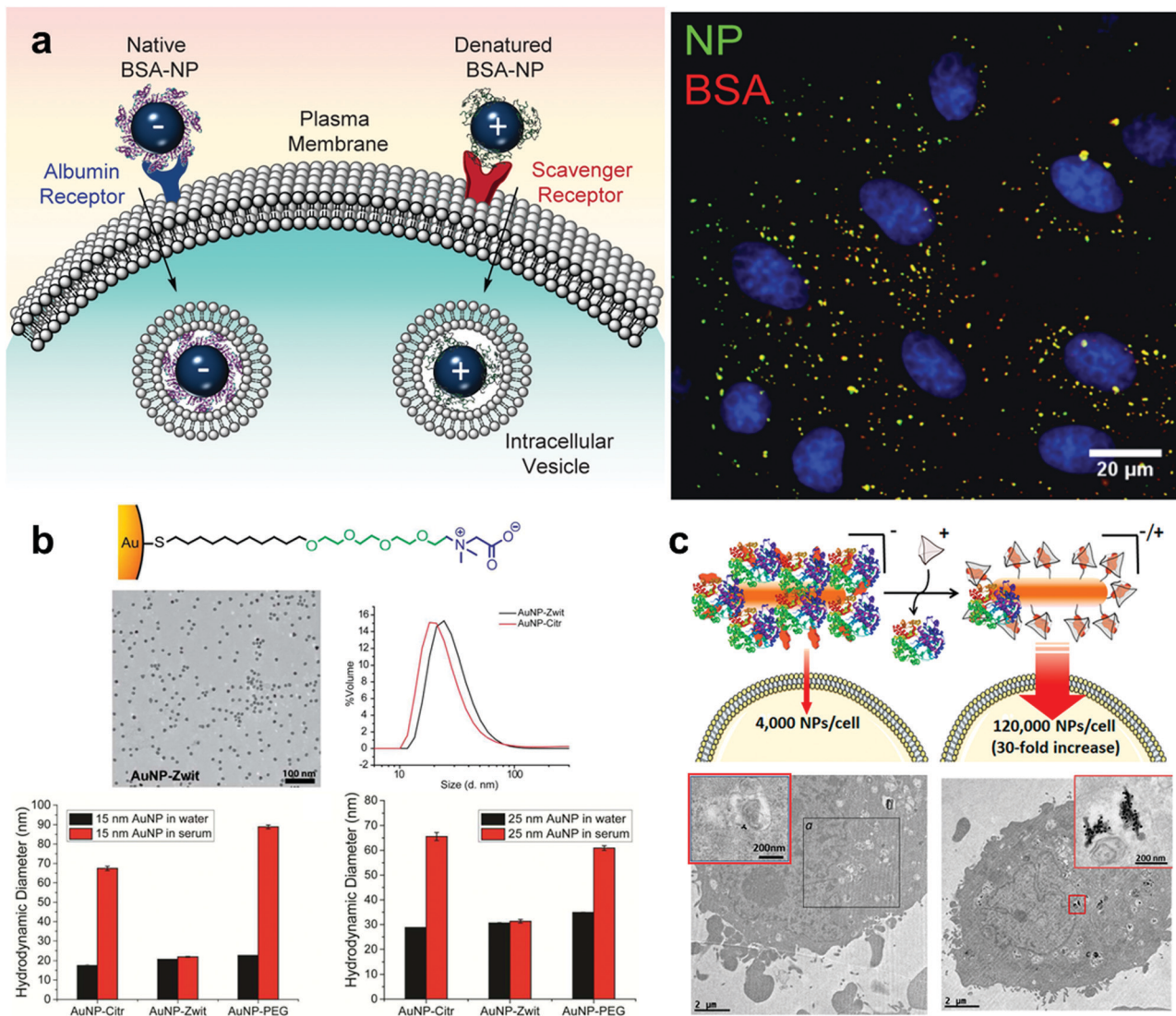


**Fig. 6** (a) The interaction between the protein corona–AuNP complex and the cell membrane. The positively and negatively charged NPs may adsorb different proteins and bind to different receptors on the cell membrane. (b) Effects of zwitterion and PEG modified nanoparticles on protein corona formation. AuNP-zwit significantly prevented the formation of a protein corona, while AuNP-PEG does the opposite. (c) The internalization of gold nanospheres NS2 in the presence or absence of cage A (in the absence or presence of a protein corona) by HeLa cells. Reproduced with permission from ref. 237, 250 and 251, copyright (2014), (2016), (2020) American Chemical Society.

building surface patterns with different properties. Among them, PEG is one of the most widely used ligands, which can effectively reduce the adsorption of non-specific proteins on the surface of AuNPs and avoid the scavenging phenomenon to some extent, extending the retention time of nanoparticles.<sup>253</sup> When the surface density of PEG reaches a high level, the protein corona formation is obviously inhibited, while AuNPs without PEG modification were detected with a higher total amount of proteins.<sup>254</sup> Moreover, AuNPs with different PEG surface densities also exhibited different cellular uptake characteristics and internalization phenomena.<sup>255</sup>

At present, most studies of protein–nanoparticle interactions focus on the homogeneous surfaces, but studies on the heterogeneous surface of nanoparticles are rare. Existing studies have demonstrated the potential of heterogeneous

surfaces in regulating protein–nanoparticle interactions. Researchers can design AuNPs with different heterogeneous surfaces to tune nanoparticle–protein interactions. In 2013, Stellacci and Lau *et al.* studied the interaction between three types of ligand-coated AuNPs ((1) all negatively charged, sulfonated alkanethiols (11-mercapto-1-undecanesulfonate, MUS), (2) a 2:1 molar mixture of MUS and 1-octanethiol (OT), and (3) a 2:1 molar mixture of MUS and a branched, apolar version of OT) and two common serum proteins (ubiquitin and fibrinogen). The results have shown that the adsorption of proteins on AuNPs is influenced by the surface heterogeneity of nanoparticles.<sup>256</sup> After that, they designed various types of AuNPs with different surface heterogeneity but the same shape, size, and composition (MUS, MUS/brOT, MUS/OT, MPA/brOT, MPA/OT). The surfaces of these nanoparticles are designed to



be randomly distributed or alternating stripe-like. They tested the interaction of these particles with protein mixtures and observed the different characteristics and behaviors of AuNPs with different surface heterogeneity when they interact with proteins.<sup>257</sup> As indicated, these studies demonstrated that tunable surface heterogeneity could be a new approach in designing nanoparticles and predicting the fate of nanoparticles.

### 5.3 Fine-tuning of the surface patterns of dendrimers to control protein adsorption

PAMAM is the first generation of dendrimers and is currently one of the most studied dendrimers. Through in-depth research over the past decades, it has been applied in many fields such as chemistry, biology, and medical treatment.<sup>258</sup> PAMAM forms a loose 3D spherical structure composed of repeating units in solution, and its core, branch units, and ends can be independently selected for flexible design.<sup>259</sup> Due to its high versatility and flexible modification, PAMAM has broad prospects for applications in drug delivery vehicles,<sup>16</sup> nucleic acid delivery vehicles,<sup>260,261</sup> and even the simulation of natural proteins.<sup>16</sup> However, the entry of PAMAM molecules without reasonable surface modifications faces the same problems as those faced by other nanoparticles (protein adsorption *via* HSA, Ig, and complement proteins and the formation of a protein corona), significantly impacting the function and fate

of nanoparticles.<sup>262–264</sup> The combination of PAMAM and HSA, which are used as drug carriers, can increase the lifetime of PAMAM in the circulation.<sup>265,266</sup>

At present, generation and surface chemical modification of dendrimers have been considered to have important effects on their protein affinity and protein corona formation.<sup>267,268</sup> Dawson *et al.* found a high correlation between the generation of cation-modified PAMAM dendrimers and cytotoxicity (Fig. 7a).<sup>269</sup> There could also be a correlation between the surface charge and particle size of PAMAM dendrimers and other health hazard events, such as platelet aggregation and thrombosis. Dobrovolskaia and Mcneil *et al.* demonstrated that large-sized cationic PAMAM dendrimers could induce platelet aggregation by interfering with the integrity of the cell membrane.<sup>270</sup> Dawson *et al.* studied the relationship between the protein corona and the relevant features of the PAMAM dendrimer using electrophotographic mobility techniques and SDS-PAGE and observed a strong interaction between the complement proteins and G6 and G7 dendrimers.<sup>271</sup>

Wang *et al.* systematically investigated the adsorption of human serum albumin (HSA), immunoglobulin (Ig), and other proteins by PAMAM dendrimers with different chemical surfaces using atomistic DMD simulations.<sup>272</sup> They used positively charged amine (NH<sub>2</sub>), negatively charged succinic acid (SA), neutral hydroxyls (OH), PEG, and photosynthate (PC) to modify the surface characteristics. This study found that these particles

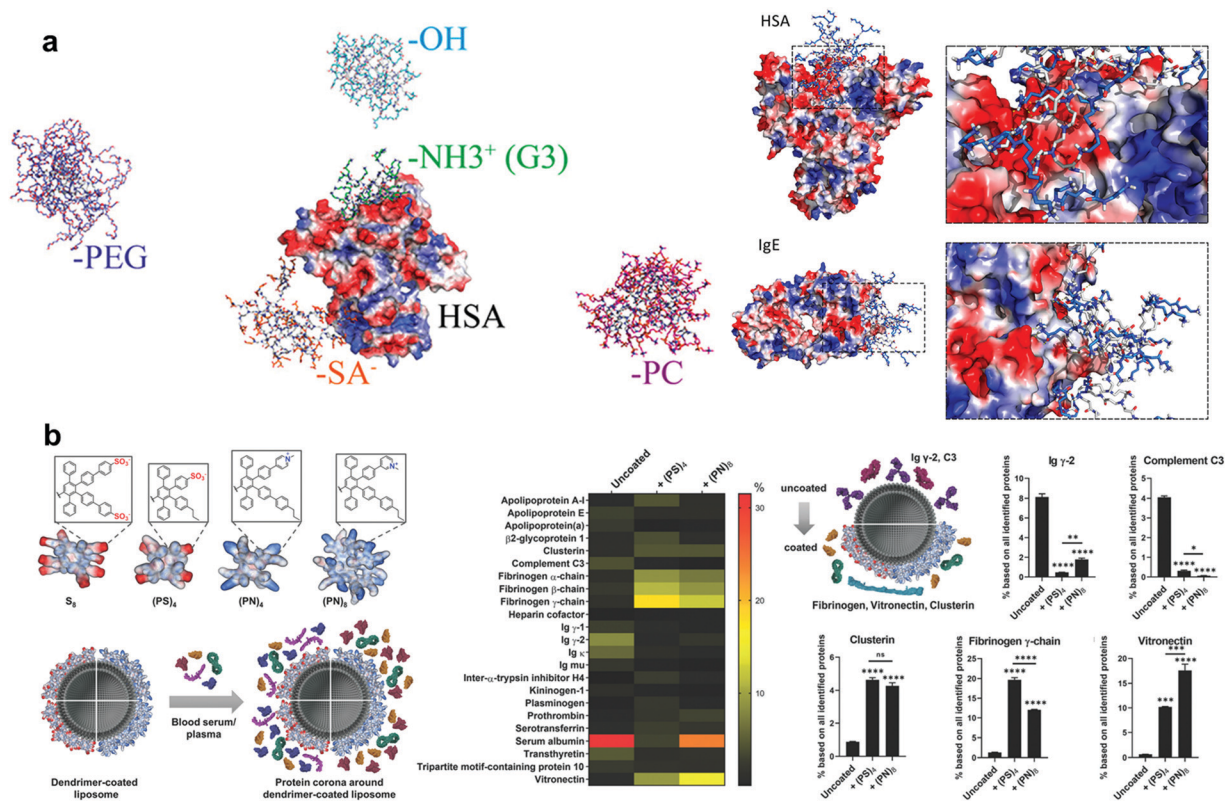


Fig. 7 (a) Snapshots of the interaction between dendritic polymers with different surface modifications and human serum proteins (HSA) from DMD simulations. (b) The comparison of protein coronas on PPD-coated liposomes and uncoated liposomes. Reproduced with permission from ref. 269 and 273, copyright (2018) American Chemical Society and (2020) The Royal Society of Chemistry.

could effectively reduce protein adsorption, while the particles on the charged surface were more likely to bind to proteins. This result may have been due to the strong electrostatic interaction between the charged PAMAM and the positively or negatively charged regions of the protein surface. This study emphasises the importance of using amphiphilic surface-modified PAMAM to prevent protein corona formation. Giri *et al.* explored the mechanism of interaction between HSA and PAMAM dendrimers. In this study, they measured the binding constants ( $K_b$ ) of a series of PAMAM molecules to HSA in a pH (7.4) aqueous solution using protein-coated silk particles. Furthermore, the researchers studied the PAMAM + HSA complex by combining <sup>1</sup>H NMR, saturation transfer difference (STD) NMR, and other methods to explore the specific mechanism of action. The results showed a correlation between the binding constant ( $K_b$ ) of PAMAM and HSA and the size of the dendrimer, as well as the chemical characteristics of the terminal group. They found that the electrostatic interaction between the charged dendrimer terminal group and the protein residue, the hydrogen bond between the internal group of the dendrimer and the protein residue, the hydrophobic interaction of nonpolar dendrimers with proteins, and the special interaction between the carboxyl group of the dendrimer and the fatty acid binding sites of HSA were the important mechanisms of adsorption of HSA by the PAMAM dendrimer.<sup>267</sup> All these results suggest the important influence of the local character difference on the interaction between the particle surface and biological environment.

PPDs are often considered to be highly hydrophobic because of their rigid structure with multiple benzene rings, and they are generally not considered to be strongly associated with biological and other neighbourhoods. However, with in-depth research in recent years, Müllen *et al.* made important contributions to the further development and biological application of PPDs. PPDs can be subjected to many precisely positioned functional modifications at different structural levels, revealing that, through reasonable preparation, modification, and functional modification, PPDs can play a key role in a series of practical biological applications.<sup>234</sup> PPDs have the characteristics of rigidity, shape durability, and accurate modification. These findings provide more possibilities and broader development prospects for in-depth research on the interaction of PPDs with biological interfaces, proteins, nucleic acids, lipids, and related practical applications.

Wagner *et al.* used a series of PPD-coated liposomal nano-carriers with different surface characteristics to explore the effects of the amphiphilic surface, surface charge, and shape durability on the adsorption of serum proteins and the formation of protein coronas. They also changed and affected the fate and orientation of liposomal nanocarriers in a biological fluid environment by controlling the surface characteristics of PPDs. They proved that the surface charge and hydrophobicity of PPDs played an important role in the formation of the liposome-protein corona, effectively reducing the adsorption of opsonin and complement proteins and inhibiting the cell uptake caused by related immune responses (Fig. 7b).<sup>273,274</sup>

These results suggest that one can control the biological characteristics of nano-drug carriers by modifying the surface of PPDs.

At present, the widely used PAMAM dendrimers often exhibit strong cytotoxicity and induce adverse immune responses.<sup>266,269</sup> Compared with PPDs, they have a flexible structure, which is likely due to the conformational rearrangement of the dendrimers that causes the special sites of surface functionalization of the dendrimers to be “folded” inward and covered, so that they cannot exert their biological or medical effects. PPDs have a rigid three-dimensional structure, a surface that can be effectively and accurately designed, and functional groups can maintain relatively accurate positions therein. The low cytotoxicity of PPDs<sup>91</sup> and other characteristics have provided broad prospects for their practical application. At present, in the related application and research field of PPDs, we believe that such macromolecules can play a more important role and have greater potential.

## 6. Surface patterns affect the interaction of nanoparticles and viruses

### 6.1 Interaction between AuNPs and viruses

Polyanionic compounds, especially polysulphate, have received increased attention due to their ability to inhibit various enveloped viruses. The polysulphate AuNPs formed by combining polysulphate with AuNPs play an effective role in virus resistance.<sup>275</sup> The mutual recognition and binding of polysulphate nanoparticles to viruses are mediated through their binding to the coat protein or capsid protein of viruses. Based on this, researchers often use polysulphate to change and modify AuNPs, making them more conducive to interaction with viruses.<sup>276,277</sup> In addition to changing the surface electrical properties of AuNPs, researchers can also modify the surface substructure using specific proteins<sup>278</sup> or aptamers<sup>279,280</sup> to allow targeted binding to viruses. For example, Chen *et al.* modified AuNPs with glucose oxidase (GOx) and concanavalin A (ConA) to interact with ConA-glycan to bind to the H3N2 virus.<sup>278</sup> Le *et al.* connected APTA MER against the purified HA protein of J1999V to AuNPs, so that J1999V was wrapped by them to form visual sedimentation and realised rapid visual detection of viruses.<sup>280</sup>

As a result, AuNPs can change their substructures through surface electrical changes and ligand modifications to further interact with the capsid protein of viruses, providing multi-purpose tools for virus detection and removal. If we could design some surface patterns for AuNPs to make them interact with viruses better or more efficiently, we not only can guide the tuning of the characteristics and functions of AuNPs, but may also obtain new compounds with unexpected effects for anti-viral therapy in the area of clinical treatment.

Setellacci *et al.* demonstrated a new anti-viral mechanism through multivalent binding which leads to an irreversible distortion of viruses through the design of ligands on the surface of nanoparticles. Strong particle binding to membranes

may result in significant local distortions. They replace the short linkers, 3-mercaptopethylsulfonate (MES), on the surface of AuNPs with long ones, undecanesulfonic acid (MUS), to achieve strong multivalent binding. *In vitro* experiments showed that MUS-AuNPs had good resistance to the viruses (Fig. 8a).<sup>281</sup> At pH 7.4, the aspartic acid and glutamic acid residues on the outer surface of the cowpea mosaic virus (CPMV) capsid protein are deprotonated and negatively charged, respectively. The polycyclic aromatic hydrocarbon (PAH)-modified AuNPs have a positive charge. Under electrostatic interactions, CPMV- and PAH-modified AuNPs can be effectively combined.<sup>282</sup> Cowpea chlorotic mottle virus (CCMV) and tobacco mosaic virus can also be combined with AuNPs *via* electrostatic interactions.<sup>283–285</sup> Although this field is in its infancy, the regulation methods are not precise enough, and AuNPs with reasonable surface patterns need to be further developed, we still believe that the concept and approaches introduced here have a chance to guide the production of medically relevant antiviral drugs.

## 6.2 Interaction between dendrimers and viruses

Dendrimers can not only be used as vectors for drugs and nucleic acids to achieve therapeutic purposes, but also for inhibiting virus-related functions. Conventional studies mainly used charges to enhance the interactions between dendrimers and viruses. For instance, dendrimers with cationic terminal

functional groups (*e.g.*, polylysine dendrimer, PAMAM) can preferentially bind to HIV envelope proteins (gp41, gp120) and related receptors (CD4 receptors) on host cells.<sup>286</sup> HIV infection involves an interaction with gp120. By blocking the formation of the CD4–gp120–chemokine receptor complex, dendrimers can hinder HIV from binding to host cells, which inhibits subsequent viral replication.<sup>287</sup> In addition, polyanionic dendrimers were also reported with anti-viral activity. Gastaminza *et al.* reported the effect of a class of polyanionic carbo silane dendrimers (PCDs) as a nanotool to control the spread of hepatitis C virus (HCV).<sup>288</sup> The anti-HCV PCD selected by them was a second-generation carbo silane dendrimer, which was G2-S24P consisting of a poly-core and a surface completely covered by 24 sulfonate groups. G2-S24P may bind to the virus envelope protein at high doses, and the electrostatic repulsion between side-chain molecules that do not participate in the electrostatic interaction with the envelope protein leads to the disruption and irreversible destabilisation of the virus envelope, during which it is likely that a large net negative charge on the surface of G2-S24P plays a key role. The broad-spectrum antiviral activity of PCDs also plays a role in the treatment of HIV and herpes simplex virus (HSV) infection, which has attracted extensive research attention.<sup>289–291</sup>

Except charges, recent studies showed that the design of proper surface patterns could allow binding of dendrimers with viruses independent of electrostatic interactions. Wu *et al.*

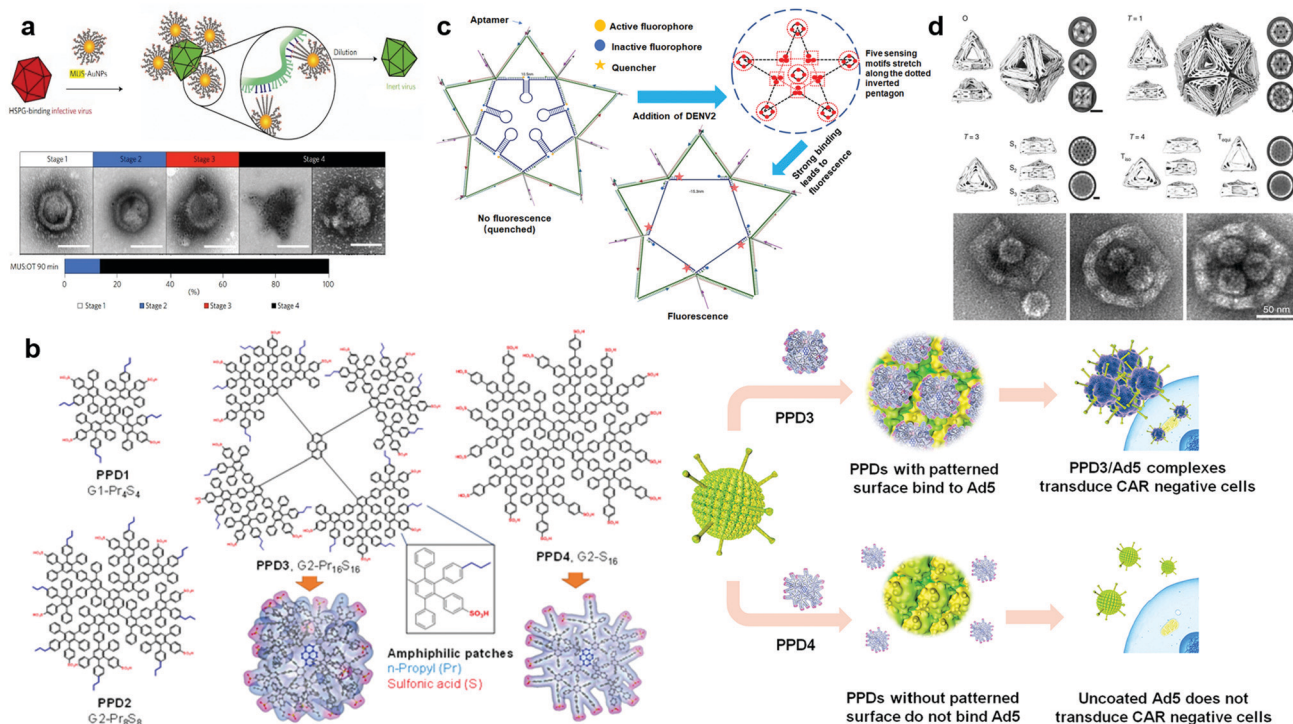


**Fig. 8** (a) Illustration and TEM images of the interaction between MUS:OT-NPs and the virus. (b) Scheme and TEM images of the course of the assembly and disassembly processes of the virus regulated by dendrons. (c) Illustration of the binding of PPDs to Ad5 and change of the transduction of Ad5. (d) Illustration and results of the detection of DENV by a star-like probe constructed by DNA. (e) Scheme of the assembly of DNA nanocages and TEM images of shells with a missing pentagon vertex engulfing up to three HBV core particles. Reproduced with permission from ref. 281, 258, 7 and 295, copyright (2017), (2020) and (2021) Springer Nature and (2019) American Chemical Society.



adopted an amphiphilic PPD with patterned alternating hydrophobic and hydrophilic groups to bind to the surface of adenovirus type 5 (Ad5) which is a common nucleic acid or drug carrier. They proved that a generation 2 PPD with a high-density amphiphilic pattern combining hydrophilic sulfonic acid groups and hydrophobic n-propyl chains could form a stable PPD/Ad5 complex. Interestingly, the mutation of the positive charges on Ad5 does not affect the binding with the amphiphilic patterned PPD, whereas the PPD with only negatively charged sulfonic acids on the surface also does not exhibit affinity with Ad5. These observations strongly supported that the binding between the PPD and Ad5 does not rely on electrostatic interactions, but most likely depends on the proper hydrophilic and hydrophobic pattern fitting with the surface structures of Ad5. The PPD binds to the Ad5 surface to form a corona structure which could also have an effect on the specific interaction of Ad5 with the cellular coxsackie-adenovirus receptor (CAR) (Fig. 8b). As a consequence, the complex showed a high transduction efficiency of Ad5 in CAR low-expression cells, which was much higher than that of Ad5 without PPD3 coating. In particular, this reduced its distribution in the liver and increased its distribution in the heart. This unique structure effectively prevented the binding of endogenous blood coagulation factor X to the virus surface because PPD masked the binding sites on the virus surface. This new idea and method of using dendrimers with amphiphilic patterns to regulate the viral vector brings more possibilities for the biomedical application of PPDs.<sup>258,274</sup>

### 6.3 Ligand patterning for virus recognition DNA based architecture interacting with viruses

DNA-based architectures are widely used for the detection and treatment of viruses because of their low toxicity and high programmability. Compared with a single ligand, the whole nanoparticle has a stronger binding capacity for the surface protein of the virus capsid after the ligand is connected to the DNA structure.<sup>292</sup> However, the distribution pattern of surface proteins of some viruses is complex, which hinders the interaction of nanoparticles with surface proteins and thus affects the recognition.<sup>293,294</sup> Therefore, it is of great significance to finely regulate the distribution of ligands in DNA structures and explore their ability to recognise viruses. One of the pioneering studies was conducted by Rinker, who provided a paradigm for exploring the effects of the spatial distribution of proteins.<sup>12</sup> In 2019, Shaw *et al.* demonstrated that the spatial distribution of antibodies on DNA origami determines the affinity between the antigen and antibody, which reaches a maximum at a distance of 16 nm.<sup>6</sup> Furthermore, Kwon *et al.* proved that, in a two-dimensional structure, the appropriate spatial distribution of ligands of specific DNA structures was necessary for the correct recognition of viruses. In their study, a “star” probe was used to detect dengue virus (DENV). A probe can bind to multiple nucleic acid aptamers. When the linked aptamer binds to the virus surface domain EDIII, its DNA structure is deformed to generate fluorescence signals. Kwon *et al.* tried three probes at different valencies (5, 6, 7) and found

that only the DNA pentagram-like star structure could detect DENV. Although the other two had more aptamers, the detection sensitivity significantly diminished (Fig. 8c).<sup>7</sup>

Additionally, in a three-dimensional structure, the spatial distribution of the ligands of the DNA structure laid the foundation for the mode of binding to the virus. Sigl *et al.* assembled a series of DNA nanocages with different numbers of subunits to isolate the invading virus from affected cells. DNA nanocages recognise viruses by the binding of antibodies on subunits to virus antigens, and the spatial distribution of antibodies is regulated by subunit topology. The virus is blocked by a semi-octahedral nanocage and a semi-decahedral with a missing pentagon vertex nanocage. Although the former can completely block viruses, the spatial distribution of the latter allows DNA nanocages to block multiple viruses simultaneously, thus having a more efficient blocking efficiency (Fig. 8d).<sup>295</sup> However, compared with the extensive research on the interaction between DNA ligand patterns and cells, research on the effect of the ligand pattern on the DNA structure on virus recognition is still rare at present.<sup>296,297</sup> Therefore, further research is required in this field.

## 7. Summary and perspective

Nanomaterials have a wide variety of sizes, morphologies, structures and surface characteristics, and their surface patterns plays a vital role in their biological effects. By adjusting and changing the surface microstructures, nanomaterials with pre-set functions can be designed. On the one hand, we hope that specially designed nanomaterials can interact with biological macromolecules, viruses, cells, *etc.* to achieve the desired biological effects. For example, the design of amphiphilic surface patterns has attracted increasing attention from researchers. Since the cell membrane has both hydrophilic and hydrophobic regions, patchy nanoparticles with alternative hydrophilic and hydrophobic patches could interact well with them, which provides an important reference for surface modification of nano-drug carriers. Similarly, the surface of the virus capsid also has hydrophilic and hydrophobic regions, and nanoparticles with a patch-like surface have a wide range of applications for the surface modification design of antiviral nano-drugs and gene therapy vectors. Dendrimers can not only provide a model for the study of protein coronas on the surface of nanoparticles, but also contribute to the field of controllable self-assembly of proteins.<sup>298</sup> Dendrimers with appropriate size and electrical properties can serve as a “bridge” for the high-ordered assembly of some cricoid proteins. Linking some ligands on the surface of nanoparticles that can interact with the surface receptors of tumor cells can improve the targeting effects of nanoparticles. Introducing groups that are responsive to light, pH and reactive oxygen species could endow nanoparticles with different electrical properties, polarities, and configurations, so as to achieve the regulation of the biological effects of nanoparticles by external conditions. For example, the chemical conformation of polymers with light-responsive



groups on the surface can be changed under light, thereby causing pores in the lipid membrane, allowing the release of drug molecules.<sup>299</sup>

On the other hand, an in-depth understanding of the biological effects of the properties of the surface patterns of nanoparticles helps to avoid the rapid removal of nanoparticles with therapeutic functions in organisms. For example, zwitterion modification reduces the formation of a protein corona on the AuNP surface which helps reduce the phagocytosis of AuNPs by opsonin-dependent immune responses. The amphiphilic PPD molecule can shield Ad5 from such molecules as antibody, complement proteins and FX in the blood, so as to prevent Ad5 from being swallowed by macrophages and endocytosed by hepatocytes.

Therefore, research on the surface patterns of nanoparticles will help researchers understand how to construct nanoparticles with different surface properties according to the expected biological effects, so as to improve the biocompatibility and targeting of nanomaterials, reduce their immunogenicity and removal, and provide a model for the biomedical application of nanomaterials. The interaction between artificial nanomaterials and biological macromolecules can provide researchers with new perspectives in the fields of molecular self-assembly and nano-machine construction, and promote the development of novel materials and methods.

## Conflicts of interest

The authors declare that they have no known competing financial interests or personal relationships that could have appeared to influence the work reported in this paper.

## Acknowledgements

This research was funded by the National Key R&D Program of China (Grant No. 2018YFA0903500), the National Natural Science Foundation of China (Grant No. 51703073) and the Open Fund from Key Laboratory of Cellular Physiology (Shanxi Medical University), Ministry of Education, China (Grant No. CPOF202103).

## References

- 1 B. Wang, L. Zhang, S. C. Bae and S. Granick, *Proc. Natl. Acad. Sci. U. S. A.*, 2008, **105**, 18171–18175.
- 2 K. Kobayashi, J. J. Wei, R. Iida, K. Ijio and K. Niikura, *Polym. J.*, 2014, **46**, 460–468.
- 3 I. M. El-Sherbiny and Y. Abbas, *Curr. Pharm. Biotechnol.*, 2016, **17**, 673–682.
- 4 H. M. Ding and Y. Q. Ma, *Nanoscale*, 2012, **4**, 1116–1122.
- 5 O. Harush-Frenkel, E. Rozentur, S. Benita and Y. Altschuler, *Biomacromolecules*, 2008, **9**, 435–443.
- 6 A. Shaw, I. T. Hoffecker, I. Smyrlaki, J. Rosa, A. Grevys, D. Bratlie, I. Sandlie, T. E. Michaelsen, J. T. Andersen and B. Hogberg, *Nat. Nanotechnol.*, 2019, **14**, 184–190.
- 7 P. S. Kwon, S. Ren, S. J. Kwon, M. E. Kizer, L. Kuo, M. Xie, D. Zhu, F. Zhou, F. M. Zhang, D. Kim, K. Fraser, L. D. Kramer, N. C. Seeman, J. S. Dordick, R. J. Linhardt, J. Chao and X. Wang, *Nat. Chem.*, 2020, **12**, 26–35.
- 8 M. Okuno, M. Mezger, R. Stangenberg, M. Baumgarten, K. Mullen, M. Bonn and E. H. Backus, *Langmuir*, 2015, **31**, 1980–1987.
- 9 S. Pogodin, N. K. H. Slater and V. A. Baulin, *ACS Nano*, 2011, **5**, 1141–1146.
- 10 Y. Gao and Y. Yu, *J. Am. Chem. Soc.*, 2013, **135**, 19091–19094.
- 11 V. P. Ma and K. Salaita, *Small*, 2019, **15**, e1900961.
- 12 S. Rinker, Y. Ke, Y. Liu, R. Chhabra and H. Yan, *Nat. Nanotechnol.*, 2008, **3**, 418–422.
- 13 M. Langecker, V. Arnaut, T. G. Martin, J. List, S. Renner, M. Mayer, H. Dietz and F. C. Simmel, *Science*, 2012, **338**, 932–936.
- 14 S. Schottler, G. Becker, S. Winzen, T. Steinbach, K. Mohr, K. Landfester, V. Mailander and F. R. Wurm, *Nat. Nanotechnol.*, 2016, **11**, 372–377.
- 15 D. C. Luther, R. Huang, T. Jeon, X. Zhang, Y. W. Lee, H. Nagaraj and V. M. Rotello, *Adv. Drug Delivery Rev.*, 2020, **156**, 188–213.
- 16 R. Esfand and D. A. Tomalia, *Drug Discovery Today*, 2001, **6**, 427–436.
- 17 A. Kusumi, C. Nakada, K. Ritchie, K. Murase, K. Suzuki, H. Murakoshi, R. S. Kasai, J. Kondo and T. Fujiwara, *Annu. Rev. Biophys. Biomol. Struct.*, 2005, **34**, 351–378.
- 18 J. M. Kalappurakkal, P. Sil and S. Mayor, *Protein Sci.*, 2020, **29**, 1355–1365.
- 19 K. Simons and M. J. Gerl, *Nat. Rev. Mol. Cell Biol.*, 2010, **11**, 688–699.
- 20 A. Verma, O. Uzun, Y. Hu, Y. Hu, H. S. Han, N. Watson, S. Chen, D. J. Irvine and F. Stellacci, *Nat. Mater.*, 2008, **7**, 588–595.
- 21 K. Jacobson, P. Liu and B. C. Lagerholm, *Cell*, 2019, **177**, 806–819.
- 22 M. Cebecauer, M. Amaro, P. Jurkiewicz, M. J. Sarmiento, R. Sachl, L. Cwiklik and M. Hof, *Chem. Rev.*, 2018, **118**, 11259–11297.
- 23 T. Fujiwara, K. Ritchie, H. Murakoshi, K. Jacobson and A. Kusumi, *J. Cell Biol.*, 2002, **157**, 1071–1081.
- 24 J. Foote and C. Milstein, *Proc. Natl. Acad. Sci. U. S. A.*, 1994, **91**, 10370–10374.
- 25 M. G. Rydahl, A. R. Hansen, S. K. Kracun and J. Mravec, *Front. Plant Sci.*, 2018, **9**, 581.
- 26 D. A. Di Giusto and G. C. King, *J. Biol. Chem.*, 2004, **279**, 46483–46489.
- 27 J. Mravec, S. K. Kracun, M. G. Rydahl, B. Westereng, D. Pontiggia, G. De Lorenzo, D. S. Domozych and W. G. T. Willats, *Plant J.*, 2017, **91**, 534–546.
- 28 K. Tanaka, K. Fukase and S. Katsumura, *Synlett*, 2011, 2115–2139.
- 29 M. R. Bond and J. J. Kohler, *Curr. Opin. Chem. Biol.*, 2007, **11**, 52–58.
- 30 J. H. Kim and E. H. Chen, *J. Cell Sci.*, 2019, **132**, jcs213124.

- 31 D. M. Lee and E. H. Chen, *Annu. Rev. Genet.*, 2019, **53**, 67–91.
- 32 F. Rodriguez-Perez, A. G. Manford, A. Pogson, A. J. Ingersoll, B. Martinez-Gonzalez and M. Rape, *Dev. Cell*, 2021, **56**, 588–601.
- 33 L. Li and F. Song, *Acta Mech. Sin.*, 2016, **32**, 970–975.
- 34 K. Kubelkova and A. Macela, *Front. Cell. Infect. Microbiol.*, 2019, **9**, 241.
- 35 A. Kusumi, K. G. Suzuki, R. S. Kasai, K. Ritchie and T. K. Fujiwara, *Trends Biochem. Sci.*, 2011, **36**, 604–615.
- 36 M. A. del Pozo, N. Balasubramanian, N. B. Alderson, W. B. Kiosses, A. Grande-Garcia, R. G. Anderson and M. A. Schwartz, *Nat. Cell Biol.*, 2005, **7**, 901–908.
- 37 T. Miclaus, C. Beer, J. Chevallier, C. Scavenius, V. E. Bochenkov, J. J. Enghild and D. S. Sutherland, *Nat. Commun.*, 2016, **7**, 11770.
- 38 T. Tanaka, A. Ogata and M. Narazaki, *Clin. Med. Insights: Ther.*, 2013, **5**, CMT.S9282.
- 39 K. Saha, M. Rahimi, M. Yazdani, S. T. Kim, D. F. Moyano, S. Hou, R. Das, R. Mout, F. Rezaee, M. Mahmoudi and V. M. Rotello, *ACS Nano*, 2016, **10**, 4421–4430.
- 40 W. H. Binder, R. Sachsenhofer, D. Farnik and D. Blaas, *Phys. Chem. Chem. Phys.*, 2008, **10**, 7328.
- 41 G. Gopalakrishnan, C. Danelon, P. Izewska, M. Prummer, P. Y. Bolinger, I. Geissbuhler, D. Demurtas, J. Dubochet and H. Vogel, *Angew. Chem., Int. Ed.*, 2006, **45**, 5478–5483.
- 42 E. Sackmann, *FEBS Lett.*, 1994, **346**, 3–16.
- 43 H. Noguchi and M. Takasu, *Biophys. J.*, 2002, **83**, 299–308.
- 44 D. Zhang, L. Wei, M. L. Zhong, L. H. Xiao, H. W. Li and J. F. Wang, *Chem. Sci.*, 2018, **9**, 5260–5269.
- 45 Y. L. Dai, C. Xu, X. L. Sun and X. Y. Chen, *Chem. Soc. Rev.*, 2017, **46**, 3830–3852.
- 46 F. Liu, D. Wu and K. Chen, *J. Nanopart. Res.*, 2014, **16**, 2556.
- 47 J. L. Tang, K. Schoenwald, D. Potter, D. White and T. Sulchek, *Langmuir*, 2012, **28**, 10033–10039.
- 48 J. Jiang, H. W. Gu, H. L. Shao, E. Devlin, G. C. Papaefthymiou and J. Y. Ying, *Adv. Mater.*, 2008, **20**, 4403–4407.
- 49 K. Davis, B. Cole, M. Ghelardini, B. A. Powell and O. T. Mefford, *Langmuir*, 2016, **32**, 13716–13727.
- 50 C. I. Mary, M. Senthilkumar and S. M. Babu, *Bull. Mater. Sci.*, 2019, **42**, 256.
- 51 T. S. Hauck, A. A. Ghazani and W. C. W. Chan, *Small*, 2008, **4**, 153–159.
- 52 Y. K. Gong and F. M. Winnik, *Nanoscale*, 2012, **4**, 360–368.
- 53 X. Liu, H. Li, Q. Jin and J. Ji, *Small*, 2014, **10**, 4230–4242.
- 54 K. Pombo Garcia, K. Zarschler, L. Barbaro, J. A. Barreto, W. O'Malley, L. Spiccia, H. Stephan and B. Graham, *Small*, 2014, **10**, 2516–2529.
- 55 D. Li, Z. Y. Miao, C. Y. Bao, X. L. Xu and Q. Zhang, *Eur. Polym. J.*, 2020, **135**, 109888.
- 56 S. Q. Qi, J. H. Sun, J. P. Ma, Y. Sun, K. Goossens, H. Li, P. Jia, X. Y. Fan, C. W. Bielawski and J. X. Geng, *Nanotechnology*, 2019, **30**, 024001.
- 57 S. Rana, A. Bajaj, R. Mout and V. M. Rotello, *Adv. Drug Delivery Rev.*, 2012, **64**, 200–216.
- 58 Y. C. Yeh, B. Creran and V. M. Rotello, *Nanoscale*, 2012, **4**, 1871–1880.
- 59 R. Sardar and J. S. Shumaker-Parry, *J. Am. Chem. Soc.*, 2011, **133**, 8179–8190.
- 60 M. Grzelczak, J. Perez-Juste, P. Mulvaney and L. M. Liz-Marzan, *Chem. Soc. Rev.*, 2008, **37**, 1783–1791.
- 61 J. Turkevich, P. C. Stevenson and J. Hillier, *Discuss. Faraday Soc.*, 1951, **11**, 55–75.
- 62 G. Frens, *Nat. Phys. Sci.*, 1973, **241**, 20–22.
- 63 Z. Babaei Afrapoli, R. Faridi Majidi, B. Negahdari and G. Tavoosidana, *Nanomed. Res. J.*, 2018, **3**, 190–196.
- 64 H. Tyagi, A. Kushwaha, A. Kumar and M. Aslam, *Nanoscale Res. Lett.*, 2016, **11**, 362.
- 65 C. Shan, H. Yang, D. Han, Q. Zhang, A. Ivaska and L. Niu, *Biosens. Bioelectron.*, 2010, **25**, 1070–1074.
- 66 E. Boisselier and D. Astruc, *Chem. Soc. Rev.*, 2009, **38**, 1759–1782.
- 67 M. Giersig and P. Mulvaney, *Langmuir*, 1993, **9**, 3408–3413.
- 68 C. A. Waters, A. J. Mills, K. A. Johnson and D. J. Schiffrin, *Chem. Commun.*, 2003, 540–541, DOI: 10.1039/B211874B.
- 69 M. Brust, M. Walker, D. Bethell, D. J. Schiffrin and R. Whyman, *J. Chem. Soc., Chem. Commun.*, 1994, 801–802, DOI: 10.1039/C39940000801.
- 70 Z. P. Guven, P. H. J. Silva, Z. Luo, U. B. Cendrowska, M. Gasbarri, S. T. Jones and F. Stellacci, *J. Visualized Exp.*, 2019, **149**, e58872.
- 71 A. M. Jackson, J. W. Myerson and F. Stellacci, *Nat. Mater.*, 2004, **3**, 330–336.
- 72 G. A. DeVries, M. Brunnbauer, Y. Hu, A. M. Jackson, B. Long, B. T. Neltner, O. Uzun, B. H. Wunsch and F. Stellacci, *Science*, 2007, **315**, 358–361.
- 73 R. J. Barsotti and F. Stellacci, *J. Mater. Chem.*, 2006, **16**, 962–965.
- 74 O. Zeiri, Y. F. Wang, A. Neyman, F. Stellacci and I. A. Weinstock, *Angew. Chem., Int. Ed.*, 2013, **52**, 968–972.
- 75 C. Singh, P. K. Ghorai, M. A. Horsch, A. M. Jackson, R. G. Larson, F. Stellacci and S. C. Glotzer, *Phys. Rev. Lett.*, 2007, **99**, 798–799.
- 76 R. P. Carney, G. A. DeVries, C. Dubois, H. Kim, J. Y. Kim, C. Singh, P. K. Ghorai, J. B. Tracy, R. L. Stiles, R. W. Murray, S. C. Glotzer and F. Stellacci, *J. Am. Chem. Soc.*, 2008, **130**, 798–799.
- 77 T. K. Mandal, M. S. Fleming and D. R. Walt, *Nano Lett.*, 2002, **2**, 3–7.
- 78 Z. Zhang, G. Sebe, X. S. Wang and K. C. Tam, *Carbohydr. Polym.*, 2018, **182**, 61–68.
- 79 Y. L. Xianyu, Z. Wang, J. S. Sun, X. F. Wang and X. Y. Jiang, *Small*, 2014, **10**, 4833–4838.
- 80 R. Raghav and S. Srivastava, *Biosens. Bioelectron.*, 2016, **78**, 396–403.
- 81 M. Larginho, R. Canto, M. Cordeiro, P. Pedrosa, A. Fortuna, R. Vinhas and P. V. Baptista, *Expert Rev. Mol. Diagn.*, 2015, **15**, 1355–1368.
- 82 R. Schreiber, I. Santiago, A. Ardavan and A. J. Turberfield, *ACS Nano*, 2016, **10**, 7303–7306.
- 83 S. H. Medina and M. E. H. El-Sayed, *Chem. Rev.*, 2009, **109**, 3141–3157.

- 84 D. Tomalia, H. Baker, J. Dewald, M. Hall, G. Kallos, S. Martin, J. Roeck, J. Ryder and P. Smith, *Polym. J.*, 1985, **17**, 117–132.
- 85 D. Tomalia, *Macromol. Symp.*, 1996, **101**, 243–255.
- 86 C. Hawker and J. Frechet, *J. Am. Chem. Soc.*, 1990, **112**, 7638–7647.
- 87 X. Feng, Y. Liang, L. Zhi, A. Thomas, D. Wu, I. Lieberwirth, U. Kolb and K. Müllen, *Adv. Funct. Mater.*, 2009, **19**, 2125–2129.
- 88 B. A. Hammer and K. Mullen, *Chem. Rev.*, 2016, **116**, 2103–2140.
- 89 T. T. Nguyen, M. Baumgarten, A. Rouhanipour, H. J. Rader, I. Lieberwirth and K. Mullen, *J. Am. Chem. Soc.*, 2013, **135**, 4183–4186.
- 90 D. Türp, T.-T.-T. Nguyen, M. Baumgarten and K. Müllen, *New J. Chem.*, 2012, **36**, 282–298.
- 91 R. Stangenberg, Y. Wu, J. Hedrich, D. Kurzbach, D. Wehner, G. Weidinger, S. L. Kuan, M. I. Jansen, F. Jelezko, H. J. Luhmann, D. Hinderberger, T. Weil and K. Müllen, *Adv. Healthcare Mater.*, 2015, **4**, 377–384.
- 92 B. A. G. Hammer, R. Moritz, R. Stangenberg, M. Baumgarten and K. Müllen, *Chem. Soc. Rev.*, 2015, **44**, 4072–4090.
- 93 B. A. G. Hammer and K. Mullen, *J. Nanopart. Res.*, 2018, **20**, 262.
- 94 P. G. d. Gennes, *Science*, 1992, **256**, 495–497.
- 95 X. T. Yu, Y. J. Sun, F. X. Liang, B. Y. Jiang and Z. Z. Yang, *Macromolecules*, 2019, **52**, 96–102.
- 96 H. Wang, W. M. Hou, Y. Z. Liu, L. Liu and H. Y. Zhao, *Macromol. Rapid Commun.*, 2021, **42**, 2000589.
- 97 G. Liu, J. Tian, X. Zhang and H. Zhao, *Chem. – Asian J.*, 2014, **9**, 2597–2603.
- 98 S. Q. Chen, C. He, H. J. Li, P. Y. Li and W. D. He, *Polym. Chem.*, 2016, **7**, 2476–2485.
- 99 J. S. J. Tan and Z. Chen, *J. Colloid Interface Sci.*, 2019, **546**, 285–292.
- 100 J. S. J. Tan, S. L. Y. Wong and Z. Chen, *Adv. Mater. Interfaces*, 2020, **7**, 1901961.
- 101 J. S. J. Tan, X. Cao, Y. Z. Huang and Z. Chen, *Colloids Surf., A*, 2020, **589**, 124460.
- 102 J. S. J. Tan, C. H. Wong and Z. Chen, *Langmuir*, 2021, **37**, 8167–8176.
- 103 D. Wu, L. Wang, W. Li, X. Xu and W. Jiang, *Int. J. Pharm.*, 2017, **533**, 169–178.
- 104 K. Halvorsen and W. P. Wong, *PLoS One*, 2012, **7**, e44212.
- 105 P. W. K. Rothmund, *Nature*, 2006, **440**, 297–302.
- 106 Y. G. Ke, S. Lindsay, Y. Chang, Y. Liu and H. Yan, *Science*, 2008, **319**, 180–183.
- 107 J. Hellmeier, R. Platzter, V. Muhlgrabner, M. C. Schneider, E. Kurz, G. J. Schutz, J. B. Huppa and E. Sevesik, *ACS Nano*, 2021, **15**, 15057–15068.
- 108 Z. L. Ge, L. J. Guo, G. Q. Wu, J. Li, Y. L. Sun, Y. Q. Hou, J. Y. Shi, S. P. Song, L. H. Wang, C. H. Fan, H. Lu and Q. Li, *Small*, 2020, **16**, e1904857.
- 109 H. T. Maune, S. P. Han, R. D. Barish, M. Bockrath, W. A. Goddard, P. W. K. Rothmund and E. Winfree, *Nat. Nanotechnol.*, 2010, **5**, 61–66.
- 110 N. V. Voigt, T. Topping, A. Rotaru, M. F. Jacobsen, J. B. Ravnsbaek, R. Subramani, W. Mamdouh, J. Kjems, A. Mokhir, F. Besenbacher and K. V. Gothelf, *Nat. Nanotechnol.*, 2010, **5**, 200–203.
- 111 Z. Liu, Z. Li, H. Zhou, G. Wei, Y. Song and L. Wang, *J. Microsc.*, 2005, **218**, 233–239.
- 112 V. V. Thacker, L. O. Herrmann, D. O. Sigle, T. Zhang, T. Liedl, J. J. Baumberg and U. F. Keyser, *Nat. Commun.*, 2014, **5**, 3448.
- 113 C. Zhou, D. Wang, Y. Dong, L. Xin, Y. Sun, Z. Yang and D. Liu, *Small*, 2015, **11**, 1161–1164.
- 114 C. Zhou, Y. Zhang, Y. Dong, F. Wu, D. Wang, L. Xin and D. Liu, *Adv. Mater.*, 2016, **28**, 9819–9823.
- 115 J. List, M. Weber and F. C. Simmel, *Angew. Chem., Int. Ed.*, 2014, **53**, 4236–4239.
- 116 Y. Suzuki, M. Endo, Y. Y. Yang and H. Sugiyama, *J. Am. Chem. Soc.*, 2014, **136**, 1714–1717.
- 117 S. Li, Q. Jiang, S. Liu, Y. Zhang, Y. Tian, C. Song, J. Wang, Y. Zou, G. J. Anderson, J. Y. Han, Y. Chang, Y. Liu, C. Zhang, L. Chen, G. Zhou, G. Nie, H. Yan, B. Ding and Y. Zhao, *Nat. Biotechnol.*, 2018, **36**, 258–264.
- 118 K. Lund, A. J. Manzo, N. Dabby, N. Michelotti, A. Johnson-Buck, J. Nangreave, S. Taylor, R. J. Pei, M. N. Stojanovic, N. G. Walter, E. Winfree and H. Yan, *Nature*, 2010, **465**, 206–210.
- 119 S. F. J. Wickham, J. Bath, Y. Katsuda, M. Endo, K. Hidaka, H. Sugiyama and A. J. Turberfield, *Nat. Nanotechnol.*, 2012, **7**, 169–173.
- 120 A. J. Thubagere, W. Li, R. F. Johnson, Z. B. Chen, S. Doroudi, Y. L. Lee, G. Izatt, S. Wittman, N. Srinivas, D. Woods, E. Winfree and L. L. Qian, *Science*, 2017, **357**, 1095.
- 121 J. V. Gregory, P. Kadiyala, R. Doherty, M. Cadena, S. Habeel, E. Ruoslahti, P. R. Lowenstein, M. G. Castro and J. Lahann, *Nat. Commun.*, 2020, **11**, 1–15.
- 122 A. E. Czapar and N. F. Steinmetz, *Curr. Opin. Chem. Biol.*, 2017, **38**, 108–116.
- 123 Q. Zhou, F. Wu, M. Wu, Y. Tian and Z. Niu, *Chem. Commun.*, 2015, **51**, 15122–15124.
- 124 J. Fueyo, R. Alemany, C. Gomez-Manzano, G. N. Fuller, A. Khan, C. A. Conrad, T. J. Liu, H. Jiang, M. G. Lemoine, K. Suzuki, R. Sawaya, D. T. Curiel, W. K. A. Yung and F. F. Lang, *J. Natl. Cancer Inst.*, 2003, **95**, 652–660.
- 125 H. Uusi-Kerttula, M. Legut, J. Davies, R. Jones, E. Hudson, L. Hanna, R. J. Stanton, J. D. Chester and A. L. Parker, *Hum. Gene Ther.*, 2015, **26**, 320–329.
- 126 L. Yu, H. Takenobu, O. Shimoizato, K. Kawamura, Y. Nimura, N. Seki, K. Uzawa, H. Tanzawa, H. Shimada, T. Ochiai and M. Tagawa, *Oncol. Rep.*, 2005, **14**, 831–835.
- 127 M. Tagawa, K. Kawamura, G. Y. Ma, Q. H. Li, Y. Takei, M. Yamanaka, M. Nakamura, Y. Tada, Y. Takiguchi, K. Tatsumi, N. Suzuki, N. Yamaguchi, K. Hiroshima and H. Shimada, *Mol. Ther.*, 2009, **17**, S235–S235.
- 128 P. Leissner, V. Legrand, Y. Schlesinger, D. A. Hadji, M. van Raaij, S. Cusack, A. Pavirani and M. Mehtali, *Gene Ther.*, 2001, **8**, 49–57.

- 129 S. A. Nicklin, E. Wu, G. R. Nemerow and A. H. Baker, *Mol. Ther.*, 2005, **12**, 384–393.
- 130 J. Kim, H. Y. Nam, T. I. Kim, P. H. Kim, J. Ryu, C. O. Yun and S. W. Kim, *Biomaterials*, 2011, **32**, 5158–5166.
- 131 P. H. Kim, J. H. Sohn, J. W. Choi, Y. Jung, S. W. Kim, S. Haam and C. O. Yun, *Biomaterials*, 2011, **32**, 2314–2326.
- 132 Y. Wan, J. F. Han, G. R. Fan, Z. R. Zhang, T. Gong and X. Sun, *Biomaterials*, 2013, **34**, 3020–3030.
- 133 C. H. Lee, D. Kasala, Y. Na, M. S. Lee, S. W. Kim, J. H. Jeong and C. O. Yun, *Biomaterials*, 2014, **35**, 5505–5516.
- 134 J. W. Choi, S. J. Jung, D. Kasala, J. K. Hwang, J. Hu, Y. H. Bae and C. O. Yun, *J. Controlled Release*, 2015, **205**, 134–143.
- 135 J. W. Choi, J. W. Park, Y. Na, S. J. Jung, J. K. Hwang, D. Choi, K. G. Lee and C. O. Yun, *Biomaterials*, 2015, **65**, 163–174.
- 136 E. C. Arvaniti, M. C. G. Juenger, S. A. Bernal, J. Duchesne, L. Courard, S. Leroy, J. L. Provis, A. Klemm and N. De Belie, *Mater. Struct.*, 2015, **48**, 3687–3701.
- 137 J. D. Clogston and A. K. Patri, in *Characterization of Nanoparticles Intended for Drug Delivery*, ed. S. E. McNeil, Humana Press, Totowa, NJ, 2011, DOI: 10.1007/978-1-60327-198-1\_6, pp. 63–70.
- 138 C. C. Guo and J. L. Yarger, *Magn. Reson. Chem.*, 2018, **56**, 1074–1082.
- 139 E. A. F. Van Doren, P. J. R. H. De Temmerman, M. A. D. Francisco and J. Mast, *J. Nanobiotechnol.*, 2011, **9**, 17.
- 140 S. Vilayurganapathy, A. Devaraj, R. Colby, A. Pandey, T. Varga, V. Shutthanandan, S. Manandhar, P. Z. El-Khoury, A. Kayani, W. P. Hess and S. Thevuthasan, *Nanotechnology*, 2013, **24**, 095707.
- 141 M. Quintana, E. Haro-Poniatowski, J. Morales and N. Batina, *Appl. Surf. Sci.*, 2002, **195**, 175–186.
- 142 A. I. Lopez-Lorente and B. Mizaikoff, *TrAC, Trends Anal. Chem.*, 2016, **84**, 97–106.
- 143 R. Abu Mukh-Qasem and A. Gedanken, *J. Colloid Interface Sci.*, 2005, **284**, 489–494.
- 144 H. Y. Zhou, X. Li, A. Lemoff, B. Zhang and B. Yan, *Analyst*, 2010, **135**, 1210–1213.
- 145 C. Jana, G. Jayamurugan, R. Ganapathy, P. K. Maiti, N. Jayaraman and A. K. Sood, *J. Chem. Phys.*, 2006, **124**, 204719.
- 146 I. S. Mashhadi, M. R. Safarnejad, M. Shahmirzaie, A. Aliahmadi and A. Ghassempour, *Anal. Chem.*, 2020, **92**, 10460–10469.
- 147 S. J. Singer and G. L. Nicolson, *Science*, 1972, **175**, 720–731.
- 148 T. Harder, P. Scheiffele, P. Verkade and K. Simons, *J. Cell Biol.*, 1998, **141**, 929–942.
- 149 K. Murase, T. Fujiwara, Y. Umemura, K. Suzuki, R. Iino, H. Yamashita, M. Saito, H. Murakoshi, K. Ritchie and A. Kusumi, *Biophys. J.*, 2004, **86**, 4075–4093.
- 150 S. M. Lu and G. D. Fairm, *Crit. Rev. Biochem. Mol. Biol.*, 2018, **53**, 192–207.
- 151 A. Kusumi, T. K. Fujiwara, R. Chadda, M. Xie, T. A. Tsunoyama, Z. Kalay, R. S. Kasai and K. G. Suzuki, *Annu. Rev. Cell Dev. Biol.*, 2012, **28**, 215–250.
- 152 S. Meinhardt and F. Schmid, *Soft Matter*, 2019, **15**, 1942–1952.
- 153 D. Lingwood and K. Simons, *Science*, 2010, **327**, 46–50.
- 154 A. L. Duncan, T. Reddy, H. Koldso, J. Helie, P. W. Fowler, M. Chavent and M. S. P. Sansom, *Sci. Rep.*, 2017, **7**, 16647.
- 155 M. A. Lemmon and J. Schlessinger, *Cell*, 2010, **141**, 1117–1134.
- 156 I. Levental, D. Lingwood, M. Grzybek, U. Coskun and K. Simons, *Proc. Natl. Acad. Sci. U. S. A.*, 2010, **107**, 22050–22054.
- 157 C. E. de Castro, J. J. Bonvent, M. C. da Silva, F. L. Castro and F. C. Giacomelli, *Macromol. Biosci.*, 2016, **16**, 1643–1652.
- 158 S. S. Sun, Y. Y. Huang, C. Zhou, S. S. Chen, M. X. Yu, J. B. Liu and J. Zheng, *Bioconjugate Chem.*, 2018, **29**, 1841–1846.
- 159 Y. C. Guo, E. Terazzi, R. Seemann, J. B. Fleury and V. A. Baulin, *Sci. Adv.*, 2016, **2**, e1600261.
- 160 M. R. Rasch, E. Rossinyol, J. L. Hueso, B. W. Goodfellow, J. Arbiol and B. A. Korgel, *Nano Lett.*, 2010, **10**, 3733–3739.
- 161 Y. Li, X. Chen and N. Gu, *J. Phys. Chem. B*, 2008, **112**, 16647–16653.
- 162 H. M. Ding, W. D. Tian and Y. Q. Ma, *ACS Nano*, 2012, **6**, 1230–1238.
- 163 L. Zhang, M. Becton and X. Wang, *J. Phys. Chem. B*, 2015, **119**, 3786–3794.
- 164 X. B. Quan, C. W. Peng, D. H. Zhao, L. B. Li, J. Fan and J. Zhou, *Langmuir*, 2017, **33**, 361–371.
- 165 J. Ma, K. Lee, J. Ban, H. Son, J. Koh, G. Hwang, H. Kim, K. Lee, M. Vang, H. Yang, H. Lim, G. Oh, S. Park and K. Yun, *J. Nanosci. Nanotechnol.*, 2013, **13**, 3801–3804.
- 166 C. Freese, M. I. Gibson, H. A. Klok, R. E. Unger and C. J. Kirkpatrick, *Biomacromolecules*, 2012, **13**, 1533–1543.
- 167 C. A. Goodman, B. L. Frankamp, B. A. Cooper and V. A. Rotello, *Colloids Surf., B*, 2004, **39**, 119–123.
- 168 E. Frohlich, *Int. J. Nanomed.*, 2012, **7**, 5577–5591.
- 169 Z. G. Yue, W. Wei, P. P. Lv, H. Yue, L. Y. Wang, Z. G. Su and G. H. Ma, *Biomacromolecules*, 2011, **12**, 2440–2446.
- 170 A. Akesson, K. M. Bendtsen, M. A. Beherens, J. S. Pedersen, V. Alfredsson and M. Cardenas Gomez, *Phys. Chem. Chem. Phys.*, 2010, **12**, 12267–12272.
- 171 A. A. Gurtovenko, J. Anwar and I. Vattulainen, *Chem. Rev.*, 2010, **110**, 6077–6103.
- 172 C. L. Ting and Z. G. Wang, *Biophys. J.*, 2011, **100**, 1288–1297.
- 173 H. Lee and R. G. Larson, *Molecules*, 2009, **14**, 423–438.
- 174 V. V. Ginzburg and S. Balijepailli, *Nano Lett.*, 2007, **7**, 3716–3722.
- 175 P. R. Leroueil, S. Y. Hong, A. Mecke, J. R. Baker, B. G. Orr and M. M. B. Holl, *Acc. Chem. Res.*, 2007, **40**, 335–342.
- 176 H. Lee and R. G. Larson, *J. Phys. Chem. B*, 2006, **110**, 18204–18211.
- 177 S. Y. Xiang, J. Wagner, T. Luckeath, K. Mullen, D. Y. W. Ng, J. Hedrich and T. Weil, *Adv. Healthcare Mater.*, 2021, 2101854.
- 178 B. A. G. Hammer, Y. Wu, S. Fischer, W. Liu, T. Weil and K. Mullen, *ChemBioChem*, 2017, **18**, 960–964.



- 179 E. C. Cho, L. Au, Q. Zhang and Y. N. Xia, *Small*, 2010, **6**, 517–522.
- 180 R. C. Van Lehn, P. U. Atukorale, R. P. Carney, Y. S. Yang, F. Stellacci, D. J. Irvine and A. Alexander-Katz, *Nano Lett.*, 2013, **13**, 4060–4067.
- 181 E. Okoampah, Y. S. Mao, S. Y. Yang, S. S. Sun and C. Zhou, *Colloids Surf., B*, 2020, **196**, 111312.
- 182 A. Akinc and G. Battaglia, *Cold Spring Harbor Perspect. Biol.*, 2013, **5**, a016980.
- 183 G. Sahay, D. Y. Alakhova and A. V. Kabanov, *J. Controlled Release*, 2010, **145**, 182–195.
- 184 W. Jiang, B. Y. S. Kim, J. T. Rutka and W. C. W. Chan, *Nat. Nanotechnol.*, 2008, **3**, 145–150.
- 185 C. Wang, B. B. Chen, M. He and B. Hu, *ACS Nano*, 2021, **15**, 3108–3122.
- 186 T. Lunnoo, J. Assawakhajornsak, S. Ruangchai and T. Puangmali, *J. Phys. Chem. B*, 2020, **124**, 1898–1908.
- 187 X. B. Quan, D. H. Zhao and J. Zhou, *Phys. Chem. Chem. Phys.*, 2021, **23**, 23526–23536.
- 188 A. M. Jackson, J. W. Myerson and F. Stellacci, *Nat. Mater.*, 2004, **3**, 330–336.
- 189 A. Verma and F. Stellacci, *Small*, 2010, **6**, 12–21.
- 190 P. Gkeka, L. Sarkisov and P. Angelikopoulos, *J. Phys. Chem. Lett.*, 2013, **4**, 1907–1912.
- 191 Y. Li, X. Li, Z. Li and H. Gao, *Nanoscale*, 2012, **4**, 3768–3775.
- 192 F. L. Tian, T. T. Yue, Y. Li and X. R. Zhang, *Sci. China: Chem.*, 2014, **57**, 1662–1671.
- 193 R. C. Van Lehn, M. Ricci, P. H. J. Silva, P. Andreozzi, J. Reguera, K. Voitchovsky, F. Stellacci and A. Alexander-Katz, *Nat. Commun.*, 2014, **5**, 4482.
- 194 N. Adachi, A. Maruyama, T. Ishihara and T. Akaike, *J. Biomater. Sci., Polym. Ed.*, 1994, **6**, 463–479.
- 195 C.-P. Tsai, C.-Y. Chen, Y. Hung, F.-H. Chang and C.-Y. Mou, *J. Mater. Chem.*, 2009, **19**, 5737–5743.
- 196 J. B. Haun and D. A. Hammer, *Langmuir*, 2008, **24**, 8821–8832.
- 197 S. Tzllil, M. Deserno, W. M. Gelbert and A. Ben-Shaul, *Biophys. J.*, 2004, **86**, 2037–2048.
- 198 G. Bao and X. R. Bao, *Proc. Natl. Acad. Sci. U. S. A.*, 2005, **102**, 9997–9998.
- 199 H. Gao, W. Shi and L. B. Freund, *Proc. Natl. Acad. Sci. U. S. A.*, 2005, **102**, 9469–9474.
- 200 H. Y. Yuan and S. L. Zhang, *Appl. Phys. Lett.*, 2010, **96**, 033704.
- 201 H. Yuan, J. Li, G. Bao and S. Zhang, *Phys. Rev. Lett.*, 2010, **105**, 138101.
- 202 Y. G. Srinivasulu, Q. F. Yao, N. Goswami and J. P. Xie, *Mater. Horiz.*, 2020, **7**, 2596–2618.
- 203 C. Dalal, A. Saha and N. R. Jana, *J. Phys. Chem. C*, 2016, **120**, 13324.
- 204 M. A. Ackun-Farmmer, K. L. Alatisse, G. Cross and D. S. W. Benoit, *Adv. Biosyst.*, 2020, **4**, e2000172.
- 205 T. K. Hart, A. M. Klinkner, J. Ventre and P. J. Bugelski, *J. Histochem. Cytochem.*, 1993, **41**, 265–271.
- 206 A. M. Wen, P. H. Rambhia, R. H. French and N. F. Steinmetz, *J. Biol. Phys.*, 2013, **39**, 301–325.
- 207 H. M. Ding and Y. Q. Ma, *Biomaterials*, 2012, **33**, 5798–5802.
- 208 V. Schubertova, F. J. Martinez-Veracoechea and R. Vacha, *Soft Matter*, 2015, **11**, 2726–2730.
- 209 L. Li, Y. Zhang and J. Wang, *R. Soc. Open Sci.*, 2017, **4**, 170063.
- 210 E. Moradi, D. Vllasaliu, M. Garnett, F. Falcone and S. Stolnik, *RSC Adv.*, 2012, **2**, 3025–3033.
- 211 A. Shaw, V. Lundin, E. Petrova, F. Fordos, E. Benson, A. Al-Amin, A. Herland, A. Blokzijl, B. Hogberg and A. I. Teixeira, *Nat. Methods*, 2014, **11**, 841–846.
- 212 T. Verheyen, T. Fang, D. Lindenhofer, Y. Wang, K. Akopyan, A. Lindqvist, B. Hogberg and A. I. Teixeira, *Nucleic Acids Res.*, 2020, **48**, 5777–5787.
- 213 K. Liu, C. Xu and J. Y. Liu, *J. Mater. Chem. B*, 2020, **8**, 6802–6809.
- 214 T. Fang, J. Alvelid, J. Spratt, E. Ambrosetti, I. Testa and A. I. Teixeira, *ACS Nano*, 2021, **15**, 3441–3452.
- 215 N. Liu, M. Tang and J. Ding, *Chemosphere*, 2020, **245**, 125624.
- 216 R. K. Mishra, A. Ahmad, A. Vyawahare, P. Alam, T. H. Khan and R. Khan, *Int. J. Biol. Macromol.*, 2021, **175**, 1–18.
- 217 H. Sun, C. Jiang, L. Wu, X. Bai and S. Zhai, *Front. Bioeng. Biotechnol.*, 2019, **7**, 414.
- 218 Y. Li, M. Girard, M. Shen, J. A. Millan and M. Olvera de la Cruz, *Proc. Natl. Acad. Sci. U. S. A.*, 2017, **114**, 11838–11843.
- 219 J. L. Kerstetter and W. M. Gramlich, *J. Mater. Chem. B*, 2014, **2**, 8043–8052.
- 220 Y. Zou, S. Ito, F. Yoshino, Y. Suzuki, L. Zhao and N. Komatsu, *ACS Nano*, 2020, **14**, 7216–7226.
- 221 S. Wilhelm, A. J. Tavares, Q. Dai, S. Ohta, J. Audet, H. F. Dvorak and W. C. W. Chan, *Nat. Rev. Mater.*, 2016, **1**, 16014.
- 222 R. Tavano, L. Gabrielli, E. Lubian, C. Fedeli, S. Visentin, P. Polverino De Laureto, G. Arrigoni, A. Geffner-Smith, F. Chen, D. Simberg, G. Morgese, E. M. Benetti, L. Wu, S. M. Moghimi, F. Mancin and E. Papini, *ACS Nano*, 2018, **12**, 5834–5847.
- 223 X. Bai, M. Xu, S. Liu and G. Hu, *ACS Appl. Mater. Interfaces*, 2018, **10**, 20368–20376.
- 224 M. S. Ehrenberg, A. E. Friedman, J. N. Finkelstein, G. Oberdorster and J. L. McGrath, *Biomaterials*, 2009, **30**, 603–610.
- 225 L. Digiaco, F. Cardarelli, D. Pozzi, S. Palchetti, M. A. Digman, E. Gratton, A. L. Capriotti, M. Mahmoudi and G. Caracciolo, *Nanoscale*, 2017, **9**, 17254–17262.
- 226 N. Feiner-Gracia, M. Beck, S. Pujals, S. Tosi, T. Mandal, C. Buske, M. Linden and L. Albertazzi, *Small*, 2017, **13**, 1701631.
- 227 M. Das, D. K. Yi and S. S. An, *Int. J. Nanomed.*, 2015, **10**, 1521–1545.
- 228 K. He, X. Liang, T. Wei, N. Liu, Y. Wang, L. Zou, J. Lu, Y. Yao, L. Kong, T. Zhang, Y. Xue, T. Wu and M. Tang, *J. Appl. Toxicol.*, 2019, **39**, 525–539.
- 229 N. Shinohara, G. Zhang, Y. Oshima, T. Kobayashi, N. Imatanaka, M. Nakai, T. Sasaki, K. Kawaguchi and M. Gamo, *Part. Fibre Toxicol.*, 2017, **14**, 48.

- 230 J. C. Y. Kah, C. Grabinski, E. Untener, C. Garrett, J. Chen, D. Zhu, S. M. Hussain and K. Hamad-Schifferli, *ACS Nano*, 2014, **8**, 4608–4620.
- 231 H. M. Ding and Y. Q. Ma, *Biomaterials*, 2014, **35**, 8703–8710.
- 232 E. Casals, T. Pfaller, A. Duschl, G. J. Oostingh and V. F. Puentes, *Small*, 2011, **7**, 3479–3486.
- 233 A. Bekdemir, S. Liao and F. Stellacci, *Colloids Surf., B*, 2019, **174**, 367–373.
- 234 R. Stangenberg, I. Saeed, S. L. Kuan, M. Baumgarten, T. Weil, M. Klapper and K. Mullen, *Macromol. Rapid Commun.*, 2014, **35**, 152–160.
- 235 N. Duran, C. P. Silveira, M. Duran and D. S. Martinez, *J. Nanobiotechnol.*, 2015, **13**, 55.
- 236 M. S. P. Boyles, T. Kristl, A. Andosch, M. Zimmermann, N. Tran, E. Casals, M. Himly, V. Puentes, C. G. Huber, U. Lutz-Meindl and A. Duschl, *J. Nanobiotechnol.*, 2015, **13**, 84.
- 237 C. C. Fleischer and C. K. Payne, *Acc. Chem. Res.*, 2014, **47**, 2651–2659.
- 238 C. D. Walkey, J. B. Olsen, H. Guo, A. Emili and W. C. Chan, *J. Am. Chem. Soc.*, 2012, **134**, 2139–2147.
- 239 W. J. Yang, K.-G. Neoh, E.-T. Kang, S. L.-M. Teo and D. Rittschof, *Prog. Polym. Sci.*, 2014, **39**, 1017–1042.
- 240 L. N. Pilon, S. P. Armes, P. Findlay and S. P. Rannard, *Langmuir*, 2005, **21**, 3808–3813.
- 241 N. Feliu, D. Docter, M. Heine, P. del Pino, S. Ashraf, J. Kolosnjaj-Tabi, P. Macchiarini, P. Nielsen, D. Alloyeau, F. Gazeau, R. H. Stauber and W. J. Parak, *Chem. Soc. Rev.*, 2016, **45**, 2440–2457.
- 242 L. Lartigue, C. Wilhelm, J. Servais, C. Factor, A. Dencausse, J. C. Bacri, N. Luciani and F. Gazeau, *ACS Nano*, 2012, **6**, 2665–2678.
- 243 J. Y. Liu and Q. A. Peng, *Acta Biomater.*, 2017, **55**, 13–27.
- 244 F. Charbgoon, M. Nejabat, K. Abnous, F. Soltani, S. M. Taghdisi, M. Alibolandi, W. T. Shier, T. W. J. Steele and M. Ramezani, *J. Controlled Release*, 2018, **272**, 39–53.
- 245 Y. Ma, J. Hong and Y. Ding, *Adv. Healthcare Mater.*, 2020, **9**, 1901448.
- 246 Z. J. Zhu, T. Posati, D. F. Moyano, R. Tang, B. Yan, R. W. Vachet and V. M. Rotello, *Small*, 2012, **8**, 2659–2663.
- 247 D. Huhn, K. Kantner, C. Geidel, S. Brandholt, I. De Cock, S. J. H. Soenen, P. R. Gil, J. M. Montenegro, K. Braeckmans, K. Mullen, G. U. Nienhaus, M. Klapper and W. J. Parak, *ACS Nano*, 2013, **7**, 3253–3263.
- 248 W. Yang, L. Zhang, S. L. Wang, A. D. White and S. Y. Jiang, *Biomaterials*, 2009, **30**, 5617–5621.
- 249 K. P. Garcia, K. Zarschler, L. Barbaro, J. A. Barreto, W. O'Malley, L. Spiccia, H. Stephan and B. Graham, *Small*, 2014, **10**, 2516–2529.
- 250 A. Gupta, D. F. Moyano, A. Parnsubsakul, A. Papadopoulos, L. S. Wang, R. F. Landis, R. Das and V. M. Rotello, *ACS Appl. Mater. Interfaces*, 2016, **8**, 14096–14101.
- 251 J. Mosquera, I. Garcia, M. Henriksen-Lacey, M. Martinez-Calvo, M. Dhanjani, J. L. Mascarenas and L. M. Liz-Marzan, *ACS Nano*, 2020, **14**, 5382–5391.
- 252 Z. F. Ma, J. Bai and X. E. Jiang, *ACS Appl. Mater. Interfaces*, 2015, **7**, 17614–17622.
- 253 E. Harrison, J. A. Coulter and D. Dixon, *Nanomedicine*, 2016, **11**, 851–865.
- 254 C. D. Walkey, J. B. Olsen, H. B. Guo, A. Emili and W. C. W. Chan, *J. Am. Chem. Soc.*, 2012, **134**, 2139–2147.
- 255 M. A. Dobrovolskaia, B. W. Neun, S. Man, X. Y. Ye, M. Hansen, A. K. Patri, R. M. Crist and S. E. McNeil, *Nanomedicine*, 2014, **10**, 1453–1463.
- 256 R. X. Huang, R. P. Carney, F. Stellacci and B. L. T. Lau, *Nanoscale*, 2013, **5**, 6928–6935.
- 257 R. X. Huang, R. R. Carney, K. Ikuma, F. Stellacci and B. L. T. Lau, *ACS Nano*, 2014, **8**, 5402–5412.
- 258 Y. Wu, L. Li, L. Frank, J. Wagner, P. Andreozzi, B. Hammer, M. D'Alicarnasso, M. Pelliccia, W. Liu, S. Chakraborty, S. Krol, J. Simon, K. Landfester, S. L. Kuan, F. Stellacci, K. Mullen, F. Kreppel and T. Weil, *ACS Nano*, 2019, **13**, 8749–8759.
- 259 E. Blundell, M. J. Healey, E. Holton, M. Sivakumaran, S. Manstana and M. Platt, *Anal. Bioanal. Chem.*, 2016, **408**, 5757–5768.
- 260 X. H. Xu, Y. T. Jian, Y. K. Li, X. Zhang, Z. X. Tu and Z. W. Gu, *ACS Nano*, 2014, **8**, 9255–9264.
- 261 Y. Dong, T. Yu, L. Ding, E. Laurini, Y. Huang, M. Zhang, Y. Weng, S. Lin, P. Chen, D. Marson, Y. Jiang, S. Giorgio, S. Pricl, X. Liu, P. Rocchi and L. Peng, *J. Am. Chem. Soc.*, 2018, **140**, 16264–16274.
- 262 G. Maiorano, S. Sabella, B. Sorce, V. Brunetti, M. A. Malvindi, R. Cingolani and P. P. Pompa, *ACS Nano*, 2010, **4**, 7481–7491.
- 263 J. Lv, C. Wang, H. Li, Z. Li, Q. Fan, Y. Zhang, Y. Li, H. Wang and Y. Cheng, *Nano Lett.*, 2020, **20**, 8600–8607.
- 264 F. Yang, Y. Zhang and H. Liang, *Int. J. Mol. Sci.*, 2014, **15**, 3580–3595.
- 265 H. Mandula, J. M. Parepally, R. Feng and Q. R. Smith, *J. Pharmacol. Exp. Ther.*, 2006, **317**, 667–675.
- 266 A. Åkesson, M. Cárdenas, G. Elia, M. P. Monopoli and K. A. Dawson, *RSC Adv.*, 2012, **2**, 11245–11248.
- 267 J. Giri, M. S. Diallo, A. J. Simpson, Y. Liu, W. A. Goddard, R. Kumar and G. C. Woods, *ACS Nano*, 2011, **5**, 3456–3468.
- 268 E. Gabellieri, G. B. Strambini, D. Shcharbin, B. Klajnert and M. Bryszewska, *Biochim. Biophys. Acta, Proteins Proteomics*, 2006, **1764**, 1750–1756.
- 269 Z. J. Deng, M. Liang, M. Monteiro, I. Toth and R. F. Minchin, *Nat. Nanotechnol.*, 2010, **6**, 39–44.
- 270 M. A. Dobrovolskaia, A. K. Patri, J. Simak, J. B. Hall, J. Semberova, S. H. De Paoli Lacerda and S. E. McNeil, *Mol. Pharmaceutics*, 2012, **9**, 382–393.
- 271 A. Åkesson, M. Cardenas, G. Elia, M. P. Monopoli and K. A. Dawson, *RSC Adv.*, 2012, **2**, 11245–11248.
- 272 B. Wang, Y. Sun, T. P. Davis, P. C. Ke, Y. Wu and F. Ding, *ACS Sustainable Chem. Eng.*, 2018, **6**, 11704–11715.
- 273 J. Wagner, M. Dillenburger, J. Simon, J. Oberlander, K. Landfester, V. Mailander, D. Y. W. Ng, K. Mullen and T. Weil, *Chem. Commun.*, 2020, **56**, 8663–8666.
- 274 J. Wagner, L. Li, J. Simon, L. Krutzke, K. Landfester, V. Mailander, K. Mullen, D. Y. W. Ng, Y. Wu and T. Weil, *Angew. Chem., Int. Ed.*, 2020, **59**, 5712–5720.

- 275 J. Vonnemann, C. Sieben, C. Wolff, K. Ludwig, C. Bottcher, A. Herrmann and R. Haag, *Nanoscale*, 2014, **6**, 2353–2360.
- 276 S. A. Staroverov, I. V. Vidyasheva, K. P. Gabalov, O. A. Vasilenko, V. N. Laskavyi and L. A. Dykman, *Bull. Exp. Biol. Med.*, 2011, **151**, 436–439.
- 277 A. S. Blum, C. M. Soto, C. D. Wilson, J. D. Cole, M. Kim, B. Gnade, A. Chatterji, W. F. Ochoa, T. W. Lin, J. E. Johnson and B. R. Ratna, *Nano Lett.*, 2004, **4**, 867–870.
- 278 C. Chen, Z. Zou, L. Chen, X. Ji and Z. He, *Nanotechnology*, 2016, **27**, 435102.
- 279 A. Halder, S. Das, D. Ojha, D. Chattopadhyay and A. Mukherjee, *Mater. Sci. Eng., C*, 2018, **89**, 413–421.
- 280 T. T. Le, B. Adamiak, D. J. Benton, C. J. Johnson, S. Sharma, R. Fenton, J. W. McCauley, M. Iqbal and A. E. G. Cass, *Chem. Commun.*, 2014, **50**, 15533–15536.
- 281 V. Cagno, P. Andreozzi, M. D'Alicarnasso, P. Jacob Silva, M. Mueller, M. Galloux, R. Le Goffic, S. T. Jones, M. Vallino, J. Hodek, J. Weber, S. Sen, E. R. Janecek, A. Bekdemir, B. Sanavio, C. Martinelli, M. Donalisio, M. A. Rameix Welti, J. F. Eleouet, Y. Han, L. Kaiser, L. Vukovic, C. Tapparel, P. Kral, S. Krol, D. Lembo and F. Stellacci, *Nat. Mater.*, 2018, **17**, 195–203.
- 282 A. A. Aljabali and D. J. Evans, *Methods Mol. Biol.*, 2014, **1108**, 97–103.
- 283 A. A. Khan, E. K. Fox, M. L. Gorzny, E. Nikulina, D. F. Brougham, C. Wege and A. M. Bittner, *Langmuir*, 2013, **29**, 2094–2098.
- 284 A. Liu, M. V. de Ruyter, S. J. Maassen and J. Cornelissen, *Methods Mol. Biol.*, 2018, **1798**, 1–9.
- 285 O. K. Zahr and A. S. Blum, *Methods Mol. Biol.*, 2014, **1108**, 105–112.
- 286 J. Peng, Z. Wu, X. Qi, Y. Chen and X. Li, *Molecules*, 2013, **18**, 7912–7929.
- 287 R. Wyatt and J. Sodroski, *Science*, 1998, **280**, 1884–1888.
- 288 D. Sepulveda-Crespo, J. L. Jimenez, R. Gomez, F. J. De La Mata, P. L. Majano, M. A. Munoz-Fernandez and P. Gastaminza, *Nanomedicine*, 2017, **13**, 49–58.
- 289 V. Briz, D. Sepulveda-Crespo, A. R. Diniz, P. Borrego, B. Rodes, F. J. de la Mata, R. Gomez, N. Taveira and M. A. Munoz-Fernandez, *Nanoscale*, 2015, **7**, 14669–14683.
- 290 L. Chonco, M. Pion, E. Vacas, B. Rasines, M. Maly, M. J. Serramia, L. Lopez-Fernandez, J. De la Mata, S. Alvarez, R. Gomez and M. A. Munoz-Fernandez, *J. Controlled Release*, 2012, **161**, 949–958.
- 291 D. Sepulveda-Crespo, M. J. Serramia, A. M. Tager, V. Vrbanc, R. Gomez, F. J. De La Mata, J. L. Jimenez and M. A. Munoz-Fernandez, *Nanomedicine*, 2015, **11**, 1299–1308.
- 292 H. Zheng, Y. Lang, J. Yu, Z. Han, B. Chen and Y. Wang, *Colloids Surf., B*, 2019, **178**, 80–86.
- 293 K. M. Ahmad, Y. Xiao and H. T. Soh, *Nucleic Acids Res.*, 2012, **40**, 11777–11783.
- 294 E. M. Strauch, S. M. Bernard, D. La, A. J. Bohn, P. S. Lee, C. E. Anderson, T. Nieuwsma, C. A. Holstein, N. K. Garcia, K. A. Hooper, R. Ravichandran, J. W. Nelson, W. Sheffler, J. D. Bloom, K. K. Lee, A. B. Ward, P. Yager, D. H. Fuller, I. A. Wilson and D. Baker, *Nat. Biotechnol.*, 2017, **35**, 667–671.
- 295 C. Sigl, E. M. Willner, W. Engelen, J. A. Kretzmann, K. Sachenbacher, A. Liedl, F. Kolbe, F. Wilsch, S. A. Aghvami, U. Protzer, M. F. Hagan, S. Fraden and H. Dietz, *Nat. Mater.*, 2021, **20**, 1281–1289.
- 296 G. A. O. Cremers, B. Rosier, A. Meijjs, N. B. Tito, S. M. J. van Duijnhoven, H. van Eenennaam, L. Albertazzi and T. F. A. de Greef, *J. Am. Chem. Soc.*, 2021, **143**, 10131–10142.
- 297 X. Liu, H. Yan, Y. Liu and Y. Chang, *Small*, 2011, **7**, 1673–1682.
- 298 H. C. Sun, L. Miao, J. X. Li, S. Fu, G. An, C. Y. Si, Z. Y. Dong, Q. Luo, S. J. Yu, J. Y. Xu and J. Q. Liu, *ACS Nano*, 2015, **9**, 5461–5469.
- 299 S. C. Sebai, S. Cribier, A. Karimi, D. Massotte and C. Tribet, *Langmuir*, 2010, **26**, 14135–14141.